frontiers in Marine Science

ORIGINAL RESEARCH
published: 28 January 2022
doi: 10.3389/fmars.2021.803439

Attributing Controlling Factors of Acidification and Hypoxia in a Deep, Nutrient-Enriched Estuarine Embayment

John R. Zeldis[1], Kim I. Currie[2], Scott L. Graham[1,3] and Mark P. Gall[4]*

[1] National Institute of Water and Atmospheric Research, Christchurch, New Zealand, [2] National Institute of Water and Atmospheric Research, Dunedin, New Zealand, [3] Manaaki Whenua – Landcare Research, Lincoln, New Zealand, [4] National Institute of Water and Atmospheric Research, Wellington, New Zealand

Measuring and attributing controlling factors of acidification and hypoxia are essential for management of coastal ecosystems affected by those stressors. We address this using surveys in the Firth of Thames, a deep, seasonally stratified estuarine embayment adjoing the Hauraki Gulf in northern Aotearoa/New Zealand. The Firth's catchment has undergone historic land-use intensification transforming it from native forest cover to dominance by pastoral use, increasing its riverine total nitrogen loading by ∼82% over natural levels and switching it's predominate loading source from offshore to the catchment. We hypothesised that seasonal variation in net ecosystem metabolism [NEM: dissolved inorganic carbon (DIC) uptake/release] will be a primary factor determining carbonate and oxic responses in the Firth, and that organic matter involved in the metabolism will originate primarily by fixation within the Firth system and be driven by catchment dissolved inorganic nitrogen (DIN) loading. Seasonal ship-based and biophysical mooring surveys across the Hauraki Gulf and Firth showed depressed pH and O_2 reaching pH ∼7.8 and O_2 ∼4.8 mg L^{-1} in autumn in the inner Firth, matched by shoreward increasing nutrient loading, phytoplankton, organic matter, gross primary production (GPP) and apparent O_2 utilization. A carbonate system deconvolution of the ship survey data, combined with other ship survey and mooring results, showed how CO_2 partial pressure responded to seasonal shifts in temperature, NEM, phytoplankton sinking and mineralisation and water column stratification, that underlay the late-season expression of acidification and hypoxia. This aligned with seasonal shifts in net DIC fluxes determined in a coincident nutrient mass-balance analysis, showing near-neutral fluxes from spring to summer, but respiratory NEM from summer to autumn. Particulate C:N and ratios of organic C fixed by Firth GPP to that from river inputs (∼29- to 100-fold in summer and autumn) showed that the dominant source of organic matter fuelling heterotrophy in autumn was autochthonous GPP, driven by riverine DIN loading. The results signified the sensitivity of deep, long-residence time, seasonally stratifying estuaries to acidification and hypoxia, and are important for coastal resource management, including aquaculture developments and catchment runoff limit-setting for maintenance of ecosystem health.

Keywords: coastal acidification, hypoxia, estuaries, primary production, nutrient loading, coastal ecosystem management, New Zealand, eutrophication

OPEN ACCESS

Edited by:
Ivica Vilibic,
Rudjer Boskovic Institute, Croatia

Reviewed by:
Jacob Carstensen,
Aarhus University, Denmark
Paul Bukaveckas,
Virginia Commonwealth University, United States

****Correspondence:***
John R. Zeldis
john.zeldis@niwa.co.nz

Specialty section:
This article was submitted to Coastal Ocean Processes, a section of the journal Frontiers in Marine Science

Received: *28 October 2021*
Accepted: *27 December 2021*
Published: *28 January 2022*

Citation:
Zeldis JR, Currie KI, Graham SL and Gall MP (2022) Attributing Controlling Factors of Acidification and Hypoxia in a Deep, Nutrient-Enriched Estuarine Embayment. Front. Mar. Sci. 8:803439. doi: 10.3389/fmars.2021.803439

INTRODUCTION

Acidification and hypoxia are now recognised as co-occurring phenomena in coastal zones worldwide (Gobler et al., 2014; Shen et al., 2019). Measuring the magnitudes of these ecosystem stressors and attributing their controlling factors are first steps toward managing and mitigating their impacts. Coastal acidification has several drivers (Duarte et al., 2013), including uptake of atmospheric CO_2 (Borges and Gypens, 2010), upwelling of historically acidified waters (Barton et al., 2012) or introductions of freshwater with differing alkalinity and pH than receiving marine waters (Osma et al., 2020). Acidification and hypoxia can also be driven by respiration of organic matter derived from primary production *in situ* or imported from land (Duarte and Prairie, 2005), thereby increasing dissolved inorganic carbon (DIC) content in coastal waters and lowering pH and O_2 (Salisbury et al., 2008; Sunda and Cai, 2012; O'Boyle et al., 2013; Wallace et al., 2014). This metabolic source has in some cases been found to be significantly outpacing other drivers of acidification (Provoost et al., 2010) and has been called the "other eutrophication problem" (Wallace et al., 2014), interacting with the O_2 depletion effects of eutrophication. The association of acidification with eutrophication indicates that extent of both stressors can be a function of catchment-derived nutrient inputs and primary production (NRC, 2000; Harding et al., 2014; Wallace et al., 2014; Testa et al., 2017; Carstensen and Duarte, 2019; Rheuban et al., 2019). The metabolic state of the system [i.e., primary production - respiration balance or Net Ecosystem Metabolism (NEM)] is thus a valuable diagnostic variable that is intimately associated with nutrient loading (Caffrey, 2004; Caffrey et al., 2014) and the important ecosystem health indicators of pH and dissolved O_2.

While NEM describes the key roles of nutrients, primary production and respiration in driving coastal acidification and hypoxia, physical and thermodynamic conditions also have important roles. Density stratification of the water column can have strong effects, by affecting CO_2 and O_2 exchange through the water column and with the atmosphere (Scully, 2016), while temperature has a strong controlling effect on CO_2 partial pressure (pCO_2) through effects on solubility and carbonate speciation (Sunda and Cai, 2012; Shen et al., 2019). Freshwater runoff with differing pH and total alkalinity (TA) compared to receiving waters, and processes including calcification, sulphate reduction and nitrate uptake can affect the expression of acidification (Wolf-Gladrow et al., 2007). Overall, it is important to understand the interactions of freshwater, NEM and physical and thermodynamic drivers, when interpreting field data or building biogeochemical models of coastal acidification and hypoxia (Rheuban et al., 2019; Shen et al., 2019).

Here we examine drivers of the carbonate and oxic environments in the Hauraki Gulf and adjoining Tikapa Moana-o-Hauraki/Firth of Thames, in northeastern Aotearoa/New Zealand (**Figure 1A**). The Hauraki Gulf (**Figure 1B**) is a large (3900 km^2, 40 m mean depth) bay lying adjacent to New Zealand's largest city, Tāmaki Makaurau/Auckland. The combined inner and outer Firth of Thames area (**Figure 1B**) is a large, deep (1100 km^2, 16 m mean depth) drowned valley estuary of the Hauraki Gulf that holds major nursery and fishing grounds for New Zealand's largest inshore fin-fishery (for snapper *Pagrus auratus*) (Zeldis and Francis, 1998; Parsons et al., 2021), some of its largest marine farms [for mussels: (Law et al., 2019)], and many recreational and cultural resources (Peart, 2016). The main rivers entering the Firth of Thames (hereafter, called the "Firth") drain the Hauraki Plains (4200 km^2) (eastern Waikato region), one of the most intensively farmed areas of New Zealand, with about 65% in pasture (mainly dairy) and about 20% in native land-cover (Vant, 2011). These rivers have been substantially nutrient-enriched over multiple decades (Snelder et al., 2017) driven by deforestation and agricultural development, including intensive draining of wetlands and peat swamps in the catchment (Judd, 2015; Kelly et al., 2020). Anthropogenic point and agricultural sources now contribute 6 and 73%, respectively, of Total N (TN) load to Hauraki Plains rivers, with "natural" sources the remainder (Vant, 2016), consistent with Snelder et al. (2017) who reported anthropogenic increases of Waikato region river TN yields of 82% over natural levels. Primary production rates in the Firth are now about double those of the seaward Hauraki Gulf (Gall and Zeldis, 2011; Zeldis and Willis, 2015), consistent with nutrient mass-balance modelling (Zeldis and Swaney, 2018) showing the Firth now receives about 85% of its dissolved inorganic nitrogen (DIN) loading from its catchment. Prior to its historic catchment land-use intensification, ocean-side nutrient loading (i.e., from the Hauraki Gulf) was likely to have contributed a much larger percentage of a much lower DIN load, to the Firth.

The valuable natural resources of the Firth, combined with recognition of its nutrient enrichment, has placed a strong focus on Firth ecosystem health by coastal resource managers and stakeholder groups, including concerns arising from observations of low pH and O_2 conditions in its waters (Law et al., 2018; Zeldis and Swaney, 2018; Kelly et al., 2020). Previous research in the Firth system has shown a strong seasonal signal in its NEM, associated with expression of low pH and O_2. It evolves from net autotrophic metabolism in spring/early summer, toward net-heterotrophic metabolism in late summer/autumn, as indicated by increasing stocks of regenerated nitrogen and phaeopigment-*a*, increases in apparent oxygen utilisation (AOU), and large late summer/autumn sags in O_2 in the lower water column (Zeldis et al., 2015). This was reflected in nutrient mass-balance analysis (Zeldis and Swaney, 2018), that showed large interseasonal swings in net DIC production in the Firth, with low net DIC production in spring and summer and high net production in autumn and winter. These findings suggested a key role of the seasonal balance of NEM in the expression of carbonate and oxic stressors in this temperate coastal system. It has been suggested (Borges and Gypens, 2010; Provoost et al., 2010) that nutrient-enrichment of coastal systems and consequent increased primary production could counter the effects of ocean acidification (i.e., from CO_2 uptake from the atmosphere). However, the seasonal fate of the fixed organic matter needs to be examined, to understand its role in expression of the stressors.

Toward this, here we examine seasonal carbonate and oxic states across the spatial gradient of freshwater and nutrient

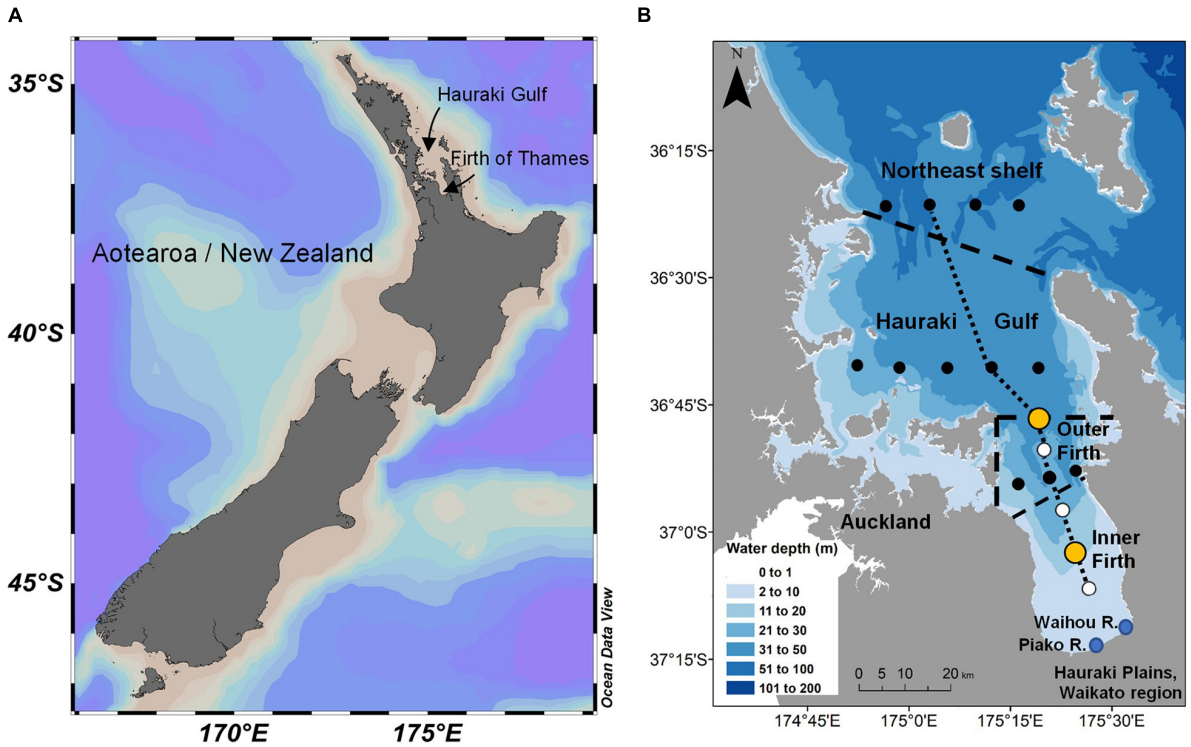

FIGURE 1 | (A) Aotearoa/New Zealand showing locations of Hauraki Gulf and adjoining Firth of Thames. **(B)** Firth of Thames ("Firth"), Hauraki Gulf and northeast shelf. Large orange circles mark the outer and inner Firth biophysical mooring sites. Black dotted sites were used for mass-balance modelling of Firth, Hauraki Gulf and northeast shelf regions, delineated by heavy dashed lines (Zeldis and Swaney, 2018). All sites were used for CTD-rosette sampling of water quality, carbonate system and fluorometer calibrations. The small dashed line delineates the inner and outer Firth regions used in **Figure 10** and **Tables 1**, **2**. The dotted line marks the transect plotted in **Figure 7**. Also labelled are Auckland city and major river mouths (Waihou and Piako rivers) entering the Firth from the Hauraki Plains in the Waikato region.

loading presented by the Firth/Hauraki Gulf system, to attribute the factors driving its carbonate and O_2 systems. We hypothesise that seasonal variation in NEM will be a primary factor determining carbonate and oxic responses in the Firth, but that its role in expression of high pCO_2 and reduced O_2 will be qualified by seasonal effects, related to temperature, nutrient limitation and physical structure. We map the carbonate and O_2 spatial fields seasonally and use high-frequency primary production data, to describe its role in the biogeochemical system. We use a deconvolution of the carbonate data to assess seasonal and spatial drivers of carbonate dynamics, and compare results with biogeochemical mass-balance modelling of the system (Zeldis and Swaney, 2018).

As a corollary to this hypothesis, we further hypothesise that the organic matter involved in metabolism will be supplied primarily by fixation within the Firth system (i.e., autochthonous), driven by catchment loading of DIN, rather than imported from the catchment as organic matter (i.e., allochthonous). This was suggested by observations of high proportions of inorganic – to – organic N loadings to the system in previous work (Zeldis and Swaney, 2018) and the dominance of that loading from the catchment with respect to DIN loading from offshore (Ibid.). Estuarine systems elsewhere have shown an opposing situation, with respiration of large contributions of allochthonous organic matter from catchments driving high DIC and low O_2 [e.g., Caffrey (2004), Salisbury et al. (2008)]. To examine this, we describe properties of organic matter in the system and estimate its autochthonous/allochthonous balance.

Addressing these hypotheses will inform how dynamic biogeochemical models of large, long-residence time, seasonally stratifying estuarine systems such as the Firth should be parameterised. We draw comparisons with other large estuaries that are showing carbonate and oxic-related stress, and discuss the sensitivity of such systems to those stressors. The findings are interpreted in the context of historic land development and nutrient runoff in the Firth region.

Their implications for coastal ecosystem resource management, including aquaculture and model forecasts of nutrient limit-settings to preserve coastal ecosystem health, are described.

MATERIALS AND METHODS

Seasonal Spatial Surveys of Carbonate and Water Quality

Carbonate system parameters (pCO_2, DIC, TA) were surveyed over the NE shelf, Hauraki Gulf and Firth (**Figure 1B**) using

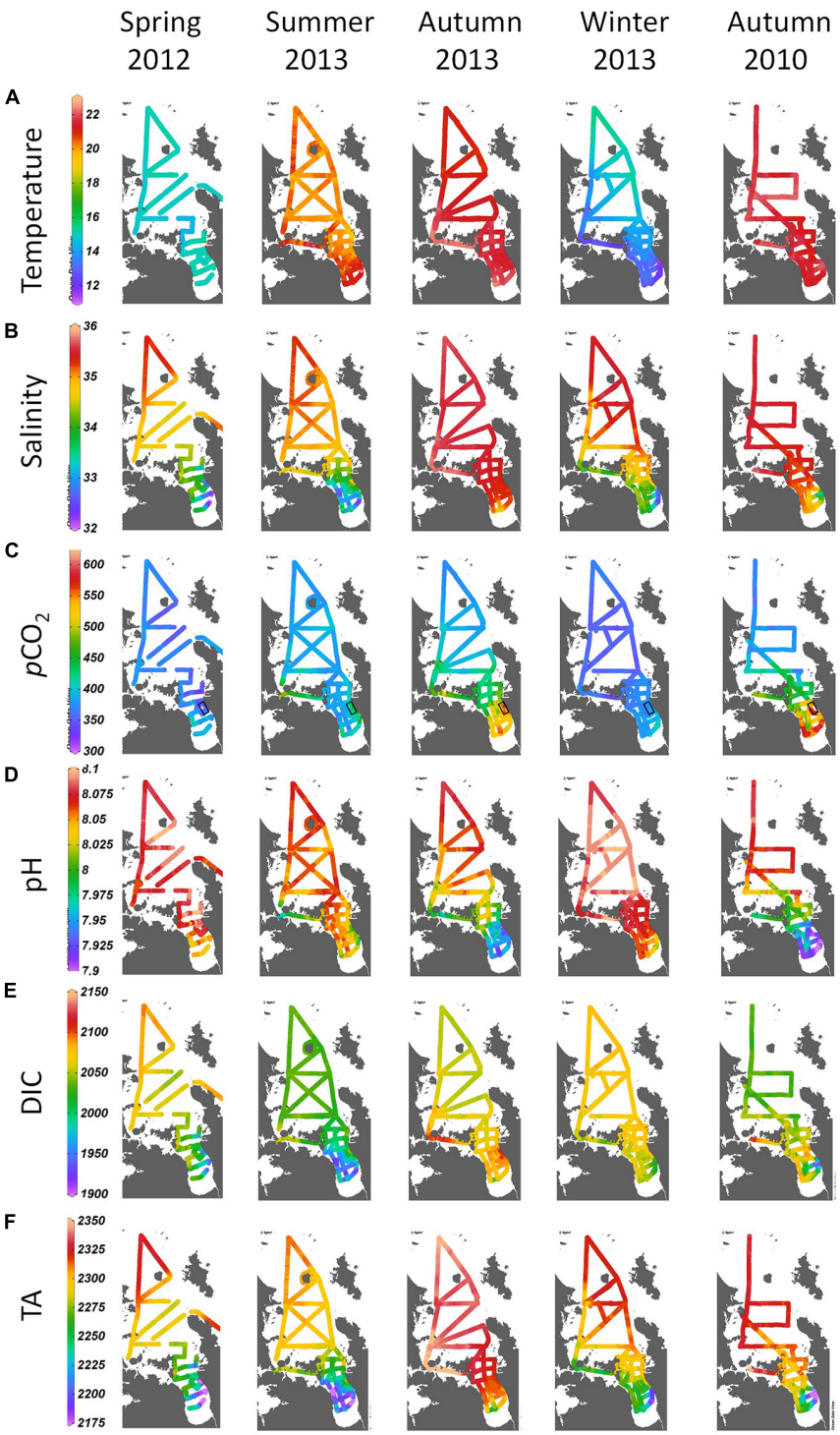

FIGURE 2 | Ribbon plots of surface layer **(A)** temperature (°C), **(B)** salinity (psu), **(C)** pCO_2 (μatm), **(D)** pH [−log(H^+)], **(E)** DIC (μmol kg^{-1}) and **(F)** TA (μmol kg^{-1}) in spring, summer, autumn and winter from underway surveys in 2012–13 and in autumn 2010 across the NE shelf, Hauraki Gulf and Firth. The black rectangle on pCO_2 plots shows the location of large mussel farms in the eastern Firth.

four seasonal ship surveys in austral spring (September), summer (December), autumn (March) and winter (July) 2012–13 (note that these surveys were not sampled consecutively in time; instead, ship scheduling logistics enforced the order: spring 2012, autumn 2013, winter 2013, summer 2013). Similar data from an earlier survey in autumn (March) 2010 were also collected.

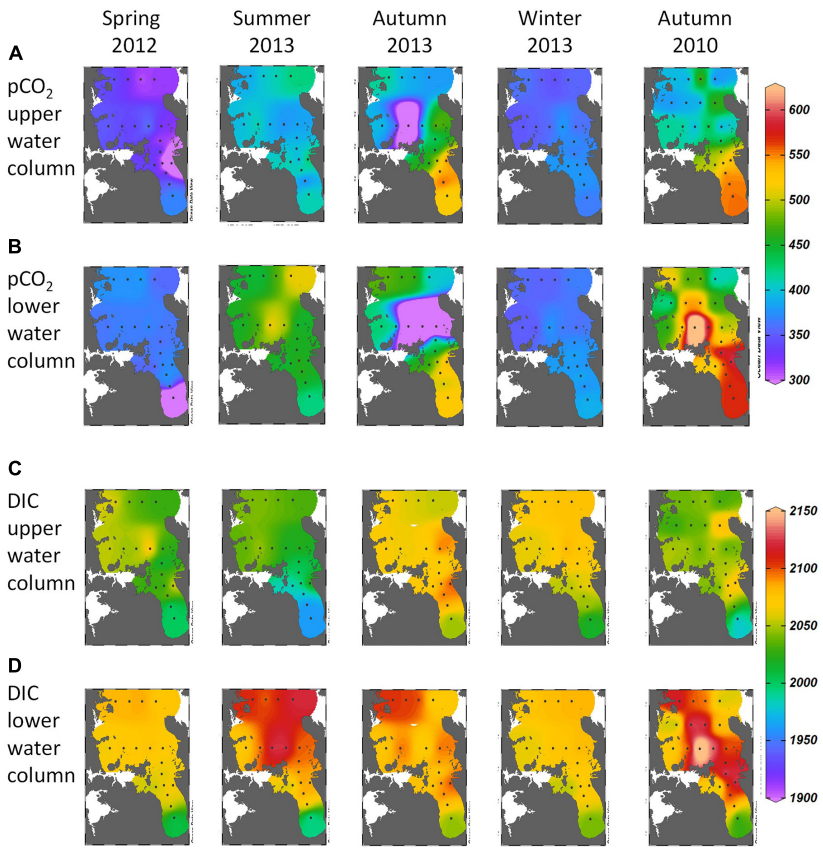

FIGURE 3 | (A,B) pCO_2 (μatm) and **(C,D)** DIC (μmol kg^{-1}) from bottle sampling in upper and lower water columns in spring, summer, autumn and winter in 2012–13 and in autumn 2010 across the Hauraki Gulf and Firth at sites indicated by dots. An additional mid-Gulf transect was occupied in autumn 2010.

Each survey used finely resolved underway mapping of the properties in the upper water column (2 m depth) using water pumped aboard the National Institute of Water and Atmosphere (NIWA) ship R.V. *Kaharoa* (28 m length) *via* a towfish and hose assembly. The seawater was delivered to a pCO_2 system where it was equilibrated with a closed air loop in a water-jacketed equilibration chamber vented to maintain atmospheric pressure in the headspace (Dickson et al., 2007). The equilibrated air was then dried and analyzed with an infrared gas analyser (IRGA, LiCor 6251), calibrated with three standard gases (NIWA gas lab, calibrated on the WMO scale) and a "zero-gas" (ambient air passed through soda lime). The pCO_2 of the equilibrated air was determined from the IRGA CO_2 mol fraction after correcting for the drying of the saturated equilibrated air, and the warming of the seawater between the surface ocean and the equilibrator. Precision of the CO_2 measurement was estimated at ±3 μatm, based on an intercalibration experiment. The 2012–13 underway sampling also included temperature, salinity (Seabird SBE21 thermo-salinograph), and fluorometric chlorophyll *a* (chl-*a*), coloured dissolved organic matter (CDOM) and turbidity (backscatter measured at 660 nm) using a Wet Labs EcoTriplet fluorometer, all sampled within the same pumped seawater stream and at the same rates as pCO_2 (10-s intervals). EcoTriplet data were not acquired in autumn 2010.

During each of the seasonal surveys the ship was stopped at 17 stations (**Figure 1B**) for discrete-depth Conductivity/Temperature/Depth (CTD)-rosette Niskin bottle (Seabird 911-rosette) profiling of the water column for physical properties (temperature, salinity, O_2), carbonate properties, chl-*a*, phaeopigment-*a* (phaeo-*a*), particulates and dissolved nutrients. Physical property sensors were factory calibrated within the interval recommended by the manufacturer (2 years) and had accuracies of 0.002°C, 0.003 mS/cm and 2% of surface O_2 saturation, respectively. Submarine light was measured as scalar photosynthetic active radiation (PAR) with an LI-194 sensor (LI-COR Inc.) mounted on the top of the CTD-rosette.

For DIC and TA, discrete samples were taken from the top (2 m depth) and near-bottom (1–2 m from bottom) 10-L rosette bottles at each CTD station. Bottles (1 L, glass) were filled following standard water sampling protocols (Dickson et al., 2007), preserved with saturated mercuric chloride and analysed within 3 months. DIC concentration was determined coulometrically using an extraction system similar to Dickson et al. (2007) with estimated accuracy and precision ± 1 μmol kg^{-1} based on the repeat analysis of Dickson Certified Reference Materials. TA was determined using a closed cell potentiometric titration (Dickson et al., 2007), and a curve fitting optimization with least squares analysis of the titration curve

(estimated accuracy and precision ± 2 μmol kg^{-1} based on the repeat Dickson Certified Reference Materials measurements). The DIC and TA data were used to calculate near-surface and near-bottom water pCO_2, using the CTD temperature, salinity and depth values and the Mehrbach dissociation constants (Mehrbach et al., 1973) as refitted by Dickson and Millero (1987). Underway near-surface TA was calculated from underway salinity using a linear relationship determined for each survey using the discrete bottle sample TA and salinity (mean $R^2 = 0.95$). Underway near-surface pH (calculated at the *in situ* temperature on the Total scale) and DIC were calculated from the measured underway pCO_2 and calculated underway TA.

Chl-*a* and phaeo-*a* profiles were taken from 2 to 6 rosette bottles per station (depending on water depth), filtered (250 mL filtrations: GFF), frozen on board (−20°C), acetone extracted in the laboratory (20 h, −18°C) and assayed on a Varian Cary Ellipse spectrofluorometer (method APHA 10200 H) before and after acidification. The near-surface chl-*a* data were used to calibrate the fluorometric chl-*a* determined on the underway surveys for each survey. The 250 mL filtrate from the chl-*a* sampling was retained for dissolved nutrient analyses, frozen on board (−20°C) in 250 mL acid-washed polyethylene bottles and assayed in the laboratory using flow injection analysis for seawater (Astoria Pacific API 300) for nitrate (NO_3^--N) and ammonium (NH_4^+-N: API methods 305-A177 and 305A026, respectively), and total dissolved N [TDN: method 10-107-04-3-B: Lachat (2010)]. Detection limits on these assays were 0.07 μmol L^{-1} for NO_3^--N and NH_4^+-N and 0.7 μmol L^{-1} for TDN.

Particulate and dissolved organic carbon and nitrogen (POC, DOC, PON, and DON, respectively) samples were collected on several seasonal surveys between 2012 and 2017 at all CTD-rosette sites from the outer Gulf (**Figure 1B**) shoreward, at near-surface and near-bottom, during seasonal surveys from R.V. *Kaharoa*, R.V. *Rangitahi III* (7.5 m length) and R.V. *Star Keys* (19.1 m length). POC and PON were determined from 250 ml filtered samples (GFF filter, precombusted) using catalytic combustion and elemental C/N analysis (method MAM, 01-190) with 0.008 and 0.007 μmol L^{-1} detection limits, respectively. DON was determined by differencing TDN with the sum of NO_3^--N and NH_4^+-N. DOC was determined from 100 ml frozen (−20°C) filtered samples (0.2 μm polycarbonate filter, direct from rosette bottles) using low level TOC analysis (method APHA5310B), with 8.3 μmol L^{-1} detection limit. Oceanographic data were visualised using Ocean Data View version 5.3.0 software (Schlitzer, 2013).

Hydrometric Data

Surface freshwater flows and nutrient loadings at coastal terminal reaches of all rivers and streams entering the Firth and Hauraki Gulf, corresponding to the 2012–13 seasonal surveys were determined by combining model estimates for unmonitored river reaches and available data for monitored reaches from NIWA and New Zealand regional council hydrometric databases. Seasonalised estimates were made using gauged daily flows for the 30 days preceding the completion date of each ocean survey, and averaged. Further details of methods used for determining freshwater and nutrient loads are available in Zeldis and Swaney (2018). Waihou River TA and pH data were acquired from the NIWA hydrometric site HM5 on the Waihou River (**Figure 1B**).

Moored Chl-*a*, Primary Production, Apparent O_2 Utilization, pH and Physical Data

An instrumented biophysical mooring acquiring fluorometric chl-*a* and submarine light data was maintained at the outer Firth site (38 m total depth: **Figure 1B**) by the aforementioned vessels over quarterly seasonal surveys between July 2005 and July 2015, using Integrating Natural Fluorometers (INF's: Biospherical) deployed at 7 and 20 m water depth. Each INF measured solar-stimulated fluorescence by phytoplankton and photosynthetic active radiation (PAR) at 15 min intervals, the ratios of which were used to estimate chl-*a* concentration at the INF depth using methods of Chamberlin et al. (1990) and Gall and Zeldis (2011). The scalar light attenuation of PAR (K_oPAR) was estimated from the difference of natural log-transformed PAR measured between the two INFs, divided by their depth difference. The fluorescence and PAR sensors were kept free of biofouling using equipment that squirted saturated bromine solution on the sensor surfaces for 15 s, every 3 h.

Further instrumented biophysical moorings were maintained at the outer and inner Firth sites (**Figure 1B**) using quarterly seasonal surveys between May 2015 and October 2017 from R.V. *Kaharoa III* and R.V. *Rangitahi*. These moorings acquired temperature, salinity, O_2 and pH data using MicroCAT (SBE-37-ODO) instruments and SeaFET pH sensors (both Sea-Bird Scientific). The MicroCAT sensors were deployed at 10 m and 35 m depth at the outer Firth and 7 m and 15 m depth at the inner Firth (17 m total depth), measuring at 15 min intervals. They were factory calibrated within the calibration interval (2 years) recommended by the manufacturer and had similar temperature, salinity and O_2 sensor accuracies as the Seabird 911 CTD instrument described above. Gross primary production (GPP) at both sites and depths was determined from the mooring O_2 data using a diel O_2 flux method (Cox et al., 2015). This method is based on the assumption that diurnal variations in O_2 are driven by GPP in response to diel solar radiation, while all other contributors to variation in O_2, such as respiration and horizontal advection, are driven by shorter (e.g., tidal) or longer (seasonal) timescale cycles. Fourier analysis was used to extract the amplitude of diurnal variations in O_2, related to autotrophic production according to Cox et al. (2015). GPP was calculated as:

$$\overline{GPP(t)} \approx 2\omega_1 \frac{sin\pi f_{DL} - cos\pi f_{DL}}{\pi f_{DL} - \frac{1}{2} sin2\pi f_{DL}} A_{O2} \quad (1)$$

where $\overline{GPP(t)}$ was average production over the time period, t, over which the Fourier amplitude, A_{O2} at the diurnal frequency, was calculated. A truncated sinusoid function of fractional daylight hours, f_{DL}, was used to approximate the effect of sunlight on diurnal patterns of GPP. Prior to Fourier analysis, data were filtered for long-term trends using a 12-h moving window average. Short gaps (< 4 h) were filled by linear interpolation. The filtered O_2 time series was then broken into 10-day blocks,

detrended linearly to remove long-term trends unrelated to daily cycles of GPP, and GPP was estimated [Eq. (1)], using the "*GPPFourier*" package of R v3.1.1 (RCoreTeam, 2014). The estimates of 10-day O_2 production by GPP (mg O_2 L^{-1} d^{-1}) were converted to carbon uptake by GPP (mg C m^{-3} d^{-1}) using the modified Redfield ratio (106 mol CO_2/ 150 mol O_2) (Anderson, 1995). One assumption of this method for GPP estimation is that there is limited air-sea exchange of O_2. Cox et al. (2015) evaluated this assumption for a range of piston velocities and turbulent diffusivities. Comparison of seasonal conditions in the Firth to these scenarios suggested that any underestimation of GPP by this method due to neglect of air-sea exchange would be within 5% (see **Supplementary Material**). For further details of the GPP calculation, assumptions involved and associated errors, see Cox et al. (2015). The mooring O_2 data were also used to calculate AOU, as the difference between saturated O_2 content and the measured O_2 content.

The SeaFET pH sensors were deployed at 4 and 5 m depth at the outer and inner biophysical moorings, respectively. They were calibrated with tris buffer before and after each deployment. From 2016 onward, the SeaFET and MicroCAT instruments at each mooring were plumbed together in the SeapHOX orientation, allowing the instruments to be operated in flow-through mode, thereby minimising biofouling and sediment deposition on the sensor surfaces. The SeaFET pH records were further calibrated using linear interpolation between deployment and recovery using bottle-determined pH values (Seabird 911-rosette) obtained upon mooring deployment and retrieval, analysed for DIC and TA as described above and using temperature and salinity data from the MicroCATs.

Deconvolution of Temperature, Metabolism and Mixing Effects on pCO_2

pCO_2 is strongly affected by water temperature, increasing it by ∼4.5% per degree of temperature increase, whereas total DIC and TA concentration are temperature invariant. Biological metabolism (uptake, release) and physical mixing (horizontal, vertical and air-sea exchanges) affect pCO_2, DIC and TA. Following the approaches of Joesoef et al. (2015) and Rosenau et al. (2021) we determined the combined effects of seasonal changes in biological metabolism and physical mixing on pCO_2. We calculated the effect of inter-seasonal temperature change on surface layer pCO_2, ($pCO_{2,thermal}$), by holding DIC and TA at observed starting seasonal conditions and imposing the observed inter-seasonal temperature changes (Mehrbach et al., 1973; Dickson and Millero, 1987). The inter-seasonal changes in DIC and TA result from metabolic and physical mixing drivers, so when evaluated at constant (initial) temperature, the calculated change in $pCO_{2,biohydro}$ will be due to those processes. Therefore the combined metabolism/mixing term was derived by the difference of the starting season pCO_2 and the pCO_2 calculated using the final season DIC, alkalinity, and salinity, and initial season temperature. Net interseasonal change of pCO_2 ($pCO_{2,net}$) was calculated as the sum of temperature ($pCO_{2,thermal}$) and combined metabolic/mixing effects ($pCO_{2,biohydro}$). The analysis was performed using averaged data for surface layer temperature, salinity, pCO_2, DIC and TA derived from the underway surveys (**Figures 2A–C,E,F**) for each seasonal transition, conducted separately for each of the inner Firth, outer Firth, Hauraki Gulf and NE shelf regions (delineated in **Figure 1B**). Differences between net pCO_2 changes thus calculated and changes in observed pCO_2 were presented as unaccounted ($pCO_{2,residual}$) change. It is likely that the relatively small unaccounted changes arose because averaging and combining their components over extensive regional areas, as done here, resulted in inconsistencies among calculation parameters.

RESULTS

Gradients of Carbonate and Biogeochemical Properties

The underway sampling (**Figure 2**) showed that in all seasons, there were shoreward increasing gradients of pCO_2 from the northeast shelf, through the Hauraki Gulf and into the Firth, and decreasing gradients of pH (**Figures 2C,D**). The gradients were weak in spring, summer and winter 2012–13, but strong in autumn 2013 when pCO_2 was greater [∼500–600 μatm and pH lower (minimum ∼7.93)] in the Firth than seaward. Further offshore over the NE shelf, pCO_2 and pH were typical of open ocean conditions (∼350–400 μatm, ∼8.05–8.10, respectively). Bottle sampling showed these pCO_2 patterns occurred in both the upper and lower water column (**Figures 3A,B**), with weak shoreward gradients in all seasons except autumn when pCO_2 maximised in the Firth.

By way of an interannual comparison, autumn 2010 had greater pCO_2 maxima (∼550–650 μatm) and lower pH minima (< 7.90) than autumn 2013 in the Firth (**Figures 2C,D**), while further seaward, values were again typical of open ocean conditions. Bottle samples showed these pCO_2 patterns occurred in both upper and lower water columns (**Figures 3A,B**).

Near-surface DIC had decreasing shoreward gradients in the underway sampling (**Figure 2E**) in all seasons except autumn, with minima in summer 2013. The near-surface bottle sampling (**Figures 3C,D**) also showed DIC minima in summer 2013, but near-bottom DIC maxima in that season. The association of these dynamics with vertical particle re-distribution will be described below.

TA (**Figure 2F**) always decreased shoreward, associated with the shoreward decreasing salinity (**Figure 2B**) toward the head of the Firth, and its major river mouths (Waihou and Piako rivers: **Figure 1B**) which together contribute the great majority of freshwater to the Firth/Hauraki Gulf system (Zeldis and Swaney, 2018) (**Figure 4A**). This pattern underlay the strong salinity – TA relationships in bottle samples used to determine underway TA from underway salinity. TA of the largest river draining to the Firth, the Waihou River was ∼230 μmol kg^{-1} (about a tenth of Firth water TA) and its pH was ∼7.2.

In spring, chl-*a* (**Figure 5A**) was evenly distributed across the northeast shelf, Hauraki Gulf and Firth, showing widespread spring phytoplankton growth that corresponded with cool temperatures (**Figure 2A**) and low pCO_2 (∼370–380 μatm;

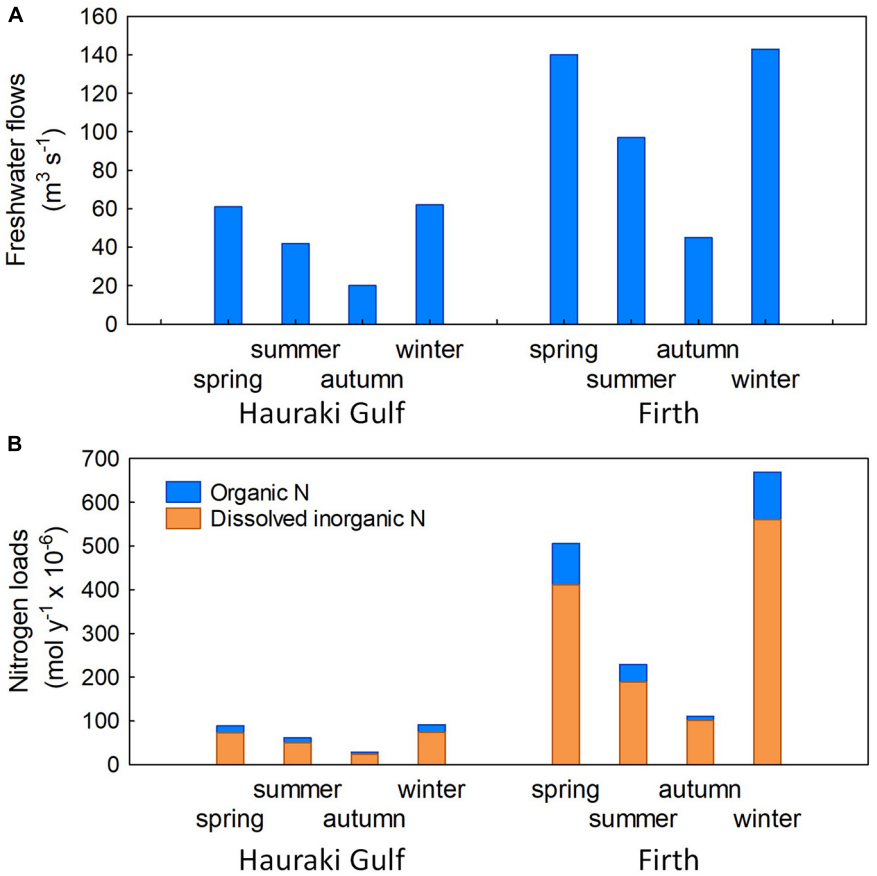

FIGURE 4 | Seasonal mean **(A)** freshwater flows (m^3 s^{-1}) and **(B)** Nitrogen (N) loads (mol y^{-1} x 10^{-6}) from rivers flowing to Hauraki Gulf and Firth during the 2012–13 seasonal surveys. The N loads are divided between dissolved inorganic N and organic N (sum of particulate and dissolved).

Figures 2C, **3A,B**). In summer and autumn, there was less chl-*a* in shelf, Hauraki Gulf and outer Firth surface waters, associated with increased temperature and pCO_2 (~400–450 μatm), while in the inner Firth, near-surface chl-*a* was elevated with maximum pCO_2 (~550–600 μatm). In winter, near-surface chl-*a* was again highest in the Firth, but also elevated across the shelf and Hauraki Gulf, associated with lowered temperature and low pCO_2 (~360–380 μatm).

Near-surface turbidity (**Figure 5B**) was highest in the Firth, in all seasons. While turbidity could be expected to trace particulate and dissolved material inputs from Firth rivers, it also indicated phytoplankton biomass originating within the Firth. This was evident in autumn, when inner Firth turbidity was maximal but river flow was least (**Figure 4A**). At that time chl-*a* in the Firth was high, (**Figure 5A**) showing correlation of phytoplankton biomass and turbidity. CDOM distribution (**Figure 5C**) closely followed the seasonal and spatial patterns of chl-*a* (elevated on the NE shelf and Hauraki Gulf in spring and winter, and higher in the Firth relative to offshore in summer, autumn and winter).

Concentrations of POC and DOC in the upper and lower water column (**Figures 6A,B**) were highest in the inner Firth and decreased seaward, following the spatial gradients in chl-*a*, turbidity and CDOM. The median molar POC:PON composition of the particulate organic matter in the Firth was 6.6 (n = 176, quartiles = 5.6–8.3), identical to the canonical Redfield ratio for phytoplankton composition (Redfield et al., 1963). The median molar DOC:DON composition of the dissolved organic matter was 11.6 (n = 160, quartiles = 9.7–14.0), somewhat above the Redfield ratio.

Further information on biogeochemical distributions was provided by depth-resolved seasonal surveys on the transect from the inner Firth to the outer Hauraki Gulf (**Figure 1B**). In all seasons except spring, chl-*a* levels were greatest in the Firth and decreased seaward (**Figure 7A**). In spring, chl-*a* and its breakdown product, phaeo-*a* (**Figure 7B**), were evenly distributed through the water column but in summer they accumulated at depth. This deepening of phytoplankton biomass in summer was indicated by increased water transmissivity in the upper column and decreased transmissivity in the lower column (**Figure 7E**). In spring, summer and autumn, NO_3^--N was depleted to low levels (≤0.5 μmol) in the upper water column (<20 m; **Figure 7C**). The deepening of the phytoplankton in summer was accompanied by intensified density stratification (**Figure 7F**) that would have exacerbated nutrient depletion in the upper water column. By autumn, stratification lessened, allowing some chl-*a* biomass increase in the upper column of the Firth.

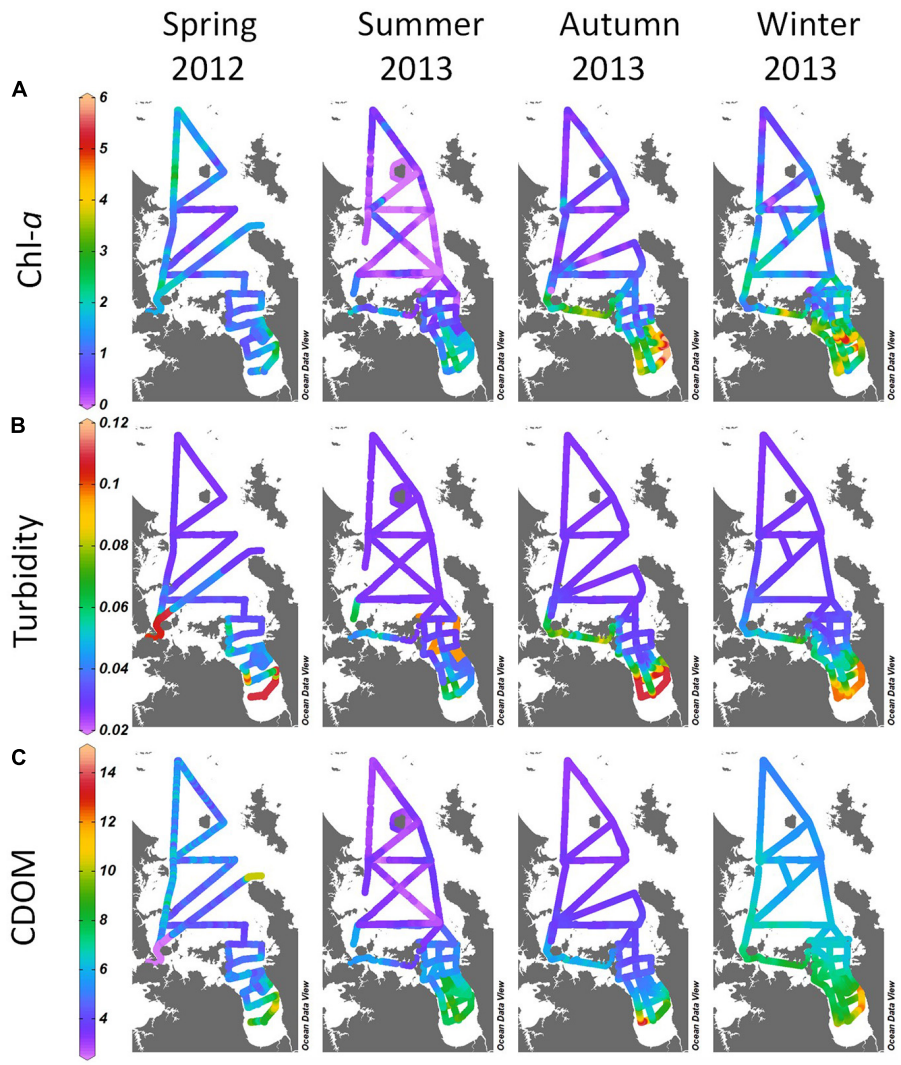

FIGURE 5 | Ribbon plots of near-surface **(A)** chlorophyll-*a* (mg m^{-3}), **(B)** turbidity [as backscatter (m^{-1} steradian^{-1})] and **(C)** coloured dissolved organic matter (CDOM: ppm) in spring, summer, autumn and winter from underway surveys in 2012-13 across the NE shelf, Hauraki Gulf and Firth.

Remineralisation of the deeply distributed biomass in summer and autumn was shown by increased NH_4^+-N and decreased O_2 concentrations in deeper Firth waters (**Figures 7D,G**).

The summer settling of phytoplankton biomass to depth and its mineralisation reflected the depletion of DIC in surface waters and increase of DIC at depth (**Figures 2E**, **3C,D**), showing that the vertical distribution of phytoplankton biomass and its nutrient-limited successional dynamics had strong influence on carbonate vertical distributions. Weakened stratification between summer and autumn (**Figure 7F**) allowed deep, low O_2 water to mix into the upper water column (**Figure 7G**). The autumn 2010 survey showed more accumulation of phytoplankton biomass at depth than autumn 2013, along with stronger stratification and lower transparency and O_2 (**Figures 7A,B,F,E,G**). This correlated with more intense pCO_2 maxima at depth in autumn 2010 than in autumn 2013 (**Figures 3A,B**).

In winter, the water column was destratified from the inner Firth seaward, and O_2 was restored to near-atmospheric levels (**Figures 7F,G**). Nitrate was also renewed (**Figure 7C**), with high values in surface waters of the inner Firth near its river mouths, that decreased seaward. Ammonium concentration was also high across the Firth in winter (**Figure 7D**) indicating mineralisation of biomass.

Settling of phytoplankton biomass in summer (**Figure 7A**) was also shown by moored fluorometer records from the outer Firth (**Figure 8**). From spring to summer, upper water column (7 m depth) chl-*a* biomass decreased, and mid-water column (20 m depth) biomass increased, indicating deepening of the chl-*a* maximum. The 20 m biomass then declined through late summer and autumn. By winter, the mid-water biomass was minimal, and upper column chl-*a* was restored. The loss of biomass from the upper column from spring to summer was indicated by decreased PAR attenuation between the two INFs

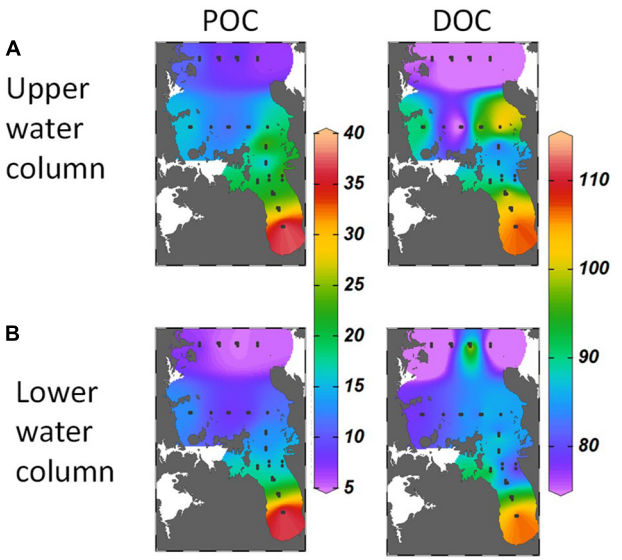

FIGURE 6 | POC, and DOC (mmol m^{-3}) in **(A)** upper and **(B)** lower water columns averaged across seasons in 2012-13, over the Hauraki Gulf and Firth at sites indicated by dots.

over that period (**Figure 8**). Light attenuation then increased in autumn as upper water column biomass was restored.

Gross Primary Production, Respiration, Mixing and pH

Firth GPP (**Figure 9A**) was described using the 2015–17 time series from the biophysical moorings at inner and outer Firth sites (**Figure 1B**). Volumetric GPP (mg C m^{-3} d^{-1}) was greater in the inner Firth than the outer Firth by 68%, averaged across seasons and water column depths (**Table 1A**). This was despite PAR light levels being 4–5 times lower in surface waters of the inner Firth (determined from CTD sampling; not shown), because of greater particulate and turbidity levels at the inner than outer Firth (**Figures 5–7**). GPP in the deeper water column at the inner Firth at 15 m was also much higher than at the outer Firth at 35 m (**Figure 9A** and **Table 1A**), even though their respective light levels were about equal, again indicating considerably more productive waters overall, at the inner Firth site.

Gross primary production (GPP) in the upper water column of the inner Firth was greatest in spring and summer, declined in autumn and was minimal in winter (**Table 1A**), and had more inter-seasonal range than GPP in the upper column of the outer Firth, where it was more consistent through the seasons. Gross primary production doubled from spring to summer in the deeper water columns of both the inner and outer Firth, corresponding with the summer deepening of their chl-*a*, transmissivity minima and light fields (**Figures 7**, **8**). The winter GPP minimum aligned with the seasonal maxima of NO_3^--N and NH_4^+-N (**Figures 7C,D**), showing the effect of decreased primary uptake on nutrient concentrations and revealing the conservative spatial pattern of NO_3^- loading from inner Firth rivers (**Figure 7C**).

Apparent oxygen utilisation (AOU) at the inner Firth site was predominately positive (**Figure 9B** and **Table 1B**), indicating consistent net-respiration. It intensified through spring into summer, near bottom. This corresponded with formation of water column stratification [as shown by density difference between the upper and lower water columns (**Figure 9D**)], indicating trapping of the O_2 – depleted water at depth. Apparent oxygen utilisation was maximal through the whole water column in autumn, when stratification broke down. At the outer Firth, upper water column AOU was either near-neutral or weakly positive, indicating metabolism more closely balanced between net-production and net-respiration. In the deeper column of the outer Firth, AOU was always positive, maximising in summer (**Table 1B**). Near-bottom AOU at the inner Firth was similar to near-bottom AOU at the outer Firth, even though the inner site was much shallower and less stratified (**Figure 9D**), indicating stronger heterotrophic metabolism at the inner Firth.

Autumn O_2 concentrations in the lower columns of both sites were often below ∼150 μmol kg^{-1} (**Figure 9C**), corresponding to ∼4.8 mg O_2 L^{-1} or ∼65% air saturation at the co-occurring temperature, salinity and barometric pressure conditions (taken as 20°C, 35.0 psu, 1013 hPa, respectively).

Upper water column pH (**Figure 9E**) was generally lower at the inner Firth than outer Firth (**Table 1C**), consistent with pH patterns in the underway surveys (**Figure 2D**). At the inner Firth these high – frequency data revealed low pH periods mainly in autumn but also in other seasons, with values often ≤7.8 and with considerably greater temporal variation than at the outer Firth. The low pH excursions at the inner Firth occurred at time scales ranging from a few days to weeks, involving multiple daily data points (themselves composed of 15 min observations) so were not considered to represent instrument errors. At the seasonal scale, strongest pH depression occurred in autumn at the inner Firth (median = 7.89: **Table 1C**), and at the outer Firth more muted depressions occurred in summer and autumn.

Deconvolution of Temperature, Metabolism and Mixing Effects on pCO_2

During the transition from spring to summer, surface layer pCO_2 increased from undersaturated levels with respect to the atmosphere to levels close to saturation (∼390 μatm in 2012–13) in all four regions (inner and outer Firth, Hauraki Gulf and NE shelf; **Table 2**). Temperatures increased substantially between spring and summer (by >5°C) across the regions, contributing a strong positive $pCO_{2,\mathrm{thermal}}$ effect (**Figure 10**). This was countered by combined metabolism/mixing that acted to lower $pCO_{2\mathrm{biohydro}}$, such that net surface layer pCO_2 ($\Delta pCO_{2,\mathrm{net}}$) increases were only moderate across the regions (∼25–33 μatm: **Figure 10** and **Table 2**). It is likely that spring GPP contributed the metabolic effect, by consuming CO_2. By summer, phytoplankton biomass had deepened and was mineralising in the lower water column (**Figures 7A,B**, **8**) beneath strong water column stratification (**Figure 7F**). Thus, between spring and summer these processes increased upper column pCO_2 while decreasing DIC (**Figures 3A,C**, **10** and **Table 2**) and increased lower water column pCO_2 and

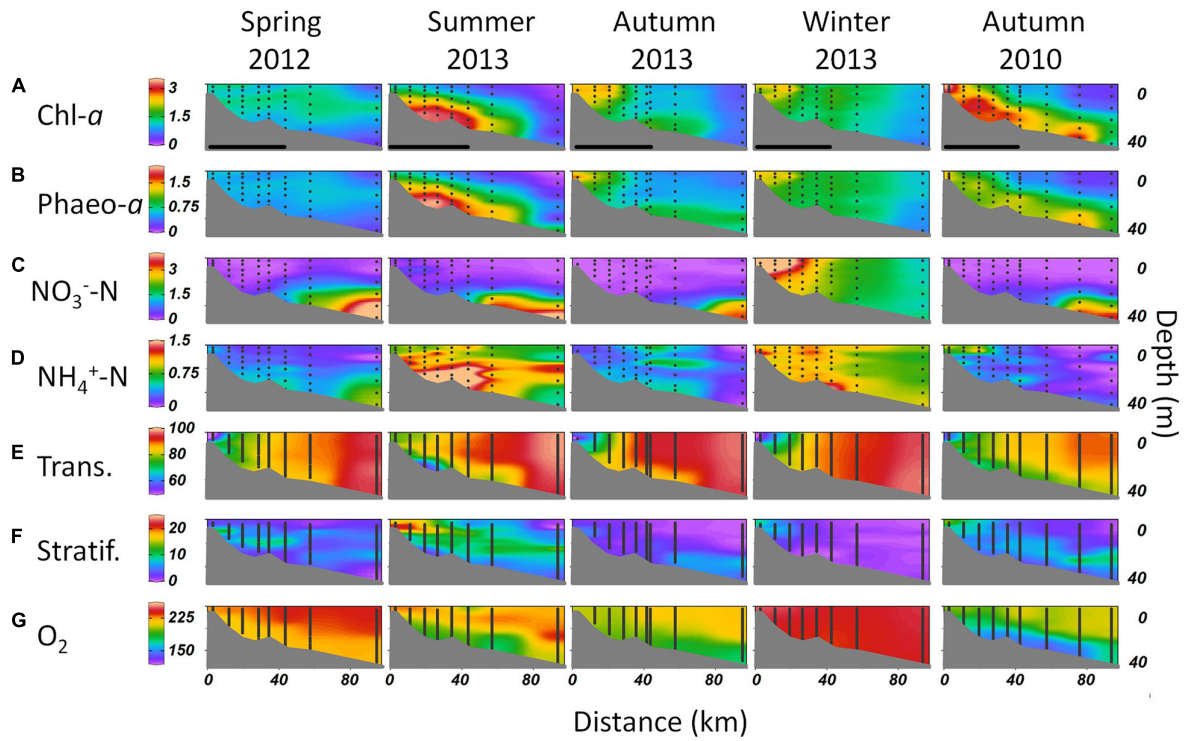

FIGURE 7 | Vertical sections of water-column properties from the inner Firth to the outer Hauraki Gulf on the transect shown in **Figure 1B**, in spring, summer, autumn, and winter 2012–13 and in autumn 2010. Properties are **(A)** chl-*a* and **(B)** phaeopigment-*a* (mg m^{-3}), **(C)** NO_3–N and **(D)** NH_{4+}-N (μmol L^{-1}), **(E)** water transmissivity (%), **(F)** stratification (Brunt Väisälä frequency, cycles h^{-1}: higher values mean more strongly stratified), and **(G)** O_2 (μmol kg^{-1}). Dots are depths of CTD bottle samples and vertical lines are 1-m interval CTD-derived values. An additional mid-Gulf station was occupied in autumn 2010. The segments in the first row show horizontal extent from the inner to the outer Firth (**Figure 1B**).

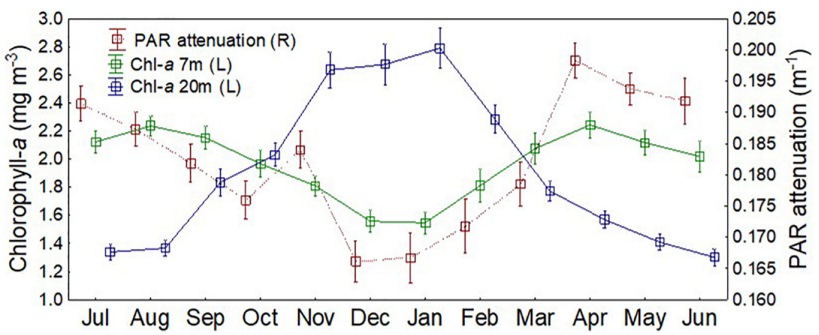

FIGURE 8 | Chl-*a* biomass **(left vertical axis)** and attenuation of photosynthetic active radiation (PAR) **(right vertical axis)** (monthly medians and quartiles), from Integrating Natural Fluorometers at the outer Firth mooring site at upper water column (7 m) and mid-water column (20) depths, determined over 2005–2015. For reference, Spring = September to November, Summer = December to February, Autumn = March to May, Winter = June to August.

DIC (**Figures 3B,D**). About 10 μatm pCO_2 change was unaccounted for by the analysis ($\Delta pCO_{2,residual}$: **Figure 10** and **Table 2**).

During the transition from summer to autumn, at the inner Firth there was a large increase of surface layer pCO_2 (122 μatm) to supersaturated levels (**Table 2**). Outer Firth pCO_2 increases were moderate (66 μatm), while Hauraki Gulf and NE shelf changes were slight and negligible, respectively. Temperature increase was small across all regions (by ≤1.6°C; **Table 2**), contributing little to the pCO_2 increases (**Figure 10**), which instead were dominated by metabolic/mixing effects. Metabolic effects were contributed by respiratory (high AOU) waters which had formed at depth in summer (**Figure 7G** and **Table 1B**). Stratification weakened in the Firth between summer and autumn (**Figure 7F**), mixing this low O_2/high AOU water toward the surface, and generating surface layer pCO_2 net increases (**Figure 10**). In the Hauraki Gulf and NE shelf regions the smaller pCO_2 increases were due to smaller metabolism/mixing effects,

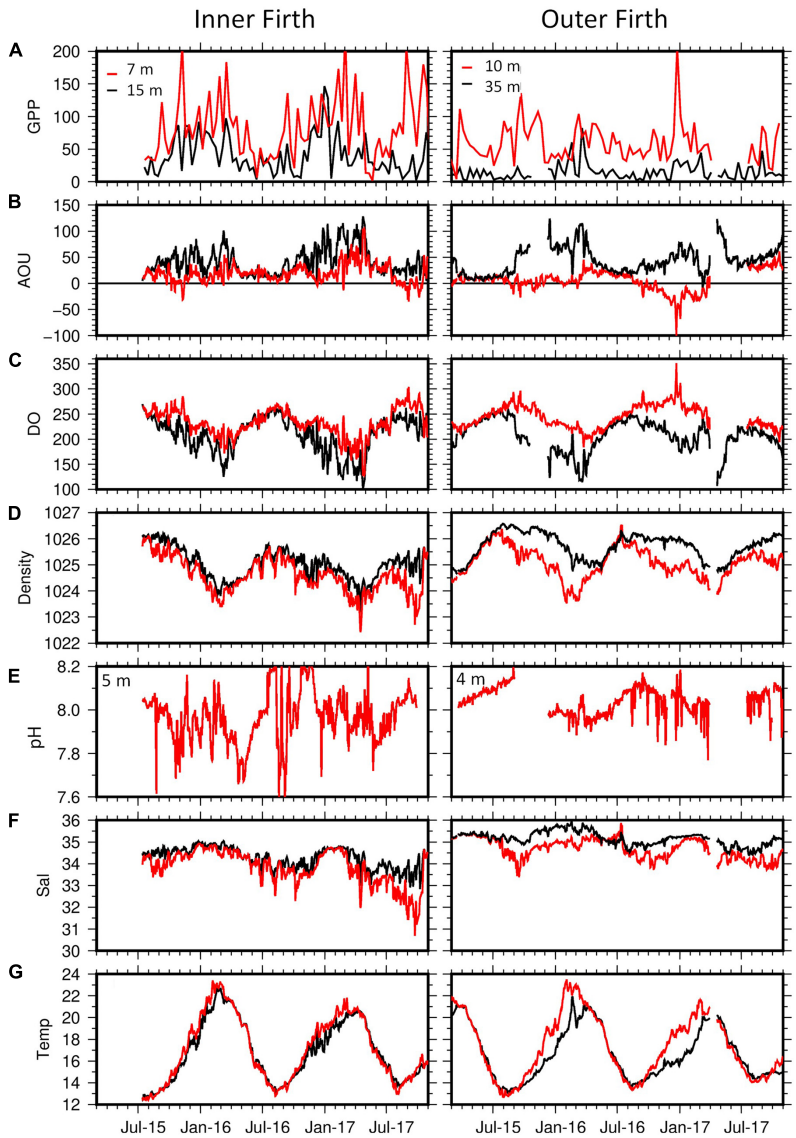

FIGURE 9 | Results from inner and outer Firth biophysical moorings (**Figure 1B**), from March 2015 to October 2017. The moorings carried temperature/salinity/O_2 sensors at upper and lower water column depths and pH sensors at upper column depths. **(A)** Gross Primary Production (mg C m^{-3} d^{-1}) from diel O_2 variation, **(B)** Apparent Oxygen Utilization (AOU: μmol kg^{-1}), **(C)** dissolved O_2 (μmol kg^{-1}), **(D)** seawater density (kg m^{-3}), **(E)** pH [−log(H^+)], **(F)** Salinity (practical salinity), **(G)** Temperature (°C). All instrument depths were as shown in **(A)** except pH, which were as shown in **(E)**. Gaps in the records were due to instrument failures.

with less phytoplankton biomass (**Figure 7A**) and more persistent stratification (**Figure 7F**). Unaccounted pCO_2 was small with respect to the net pCO_2 increases at the inner Firth, outer Firth and Hauraki Gulf, but was of similar magnitude to the small net changes at the NE shelf.

In the transition from autumn to winter, there was a large decrease of inner Firth surface layer pCO_2 (138 μatm: **Table 2**), moderate decrease at the outer Firth (82 μatm) and small decreases at Hauraki Gulf and NE shelf, reducing pCO_2 to below atmospheric equilibrium in all regions. Temperatures decreased strongly in all regions (by ∼7.6°C: **Table 2**) with strong reducing effects on pCO_2, while metabolic/mixing processes had increasing effects on pCO_2 (**Figure 10**). The temperature effect was strongest at the inner Firth because its shallow waters have a larger annual temperature range than further offshore (**Table 2**), due to proximity to terrestrial seasonal heating and cooling. Heterotrophic metabolism effects were enhanced by low (light-limited) winter GPP (**Table 1A**), indicated also by high winter NO_3^--N and NH_4^+-N levels (**Figures 7C,D**). Mixing effects were contributed by complete breakdown of stratification in the outer Firth, Hauraki Gulf and NE shelf (**Figure 7F**), favouring CO_2 equilibration with the atmosphere. An average of ∼15 μatm pCO_2 was unaccounted for.

From winter to spring, surface layer pCO_2 changed little in all regions, remaining near or below equilibrium with the atmosphere (**Table 2**). Sea temperatures increased only slightly

TABLE 1 | Seasonal medians for biophysical mooring data, at inner and outer Firth sites (**Figure 1B**) for (A) Gross Primary Production (GPP: mg C m^{-3} d^{-1}), (B) Apparent Oxygen Utilisation (AOU: μmol O_2 kg^{-1}) at upper and lower water column depths (m) and (C) pH [- log(H^+)] at upper water column depths.

	(A) GPP				(B) AOU				(C) pH	
Sites	**Inner Firth**		**Outer Firth**		**Inner Firth**		**Outer Firth**		**Inner Firth**	**Outer Firth**
Depths	**7 m**	**15 m**	**10 m**	**35 m**	**7 m**	**15 m**	**10 m**	**35 m**	**5 m**	**4 m**
Spring	83 a	32 a	67 a	10 a	14 a	39 a	0 a	52 a	8.01 a	8.08 a
Summer	95 a	65 b	45 a	22 b	15 a	56 b	−6 b	64 b	7.99 a	7.99 b
Autumn	76 a, b	34 a, b	56 a	12 a, b	32 b	56 b	10 c	36 c	7.89 b	8.02 b
Winter	41 b	22 a	46 a	8 a	15 a	22 c	14 d	23 d	8.00 a	8.08 a

Seasonal values with different letters were significantly different ($p < 0.05$; Kruskal Wallis multiple comparisons). Seasons were austral spring: September-November, summer: December-February, autumn: March-May, winter: June-August.

across the regions (∼1°C) and effects due to metabolism/mixing were slight, such that $\Delta pCO_{2,net}$ changed little (**Figure 10**).

Overall, the region with largest net inter-seasonal variations in surface layer pCO_2 was the inner Firth. This included strong pCO_2 increase from summer to autumn, little of which was attributable to increased temperature, but resulted from mixing of deeper, highly respiratory waters that had formed in summer toward the surface. Between autumn and winter, pCO_2 decreased in all regions, driven by large temperature decrease. In the outer Firth, seasonal net pCO_2 variations were more moderate, while at Hauraki Gulf and NE shelf they were relatively slight.

DISCUSSION

Attributing Factors Controlling Carbonate and Oxygen Variation

Resolving and disentangling the relative contributions of factors controlling acidification and hypoxia is important for understanding their current states, and for developing models useful for forecasting and mitigating their effects [e.g., Rheuban et al. (2019), Shen et al. (2019)]. Our study has approached this using finely resolved spatial surveys of physical, carbonate and biogeochemical observations from ship surveys, and temporally intensive primary production, O_2 and physical data from fixed biophysical moorings, combined with a deconvolution of controlling factors.

While uptake of atmospheric CO_2 by the open ocean since the industrial revolution has had a clear impact on its pH, decreasing it by ∼0.1 unit and raising its pCO_2 by ∼100 uatm (Duarte et al., 2013), our work shows that these changes will have made relatively small contributions to the wide variations in carbonate conditions in inshore waters of the Hauraki Gulf and especially the Firth. We observed the NE shelf region to have pCO_2 at near-equilibrium or slightly below atmospheric levels and pH close to 8.1, with little seasonal variability, but larger pCO_2 and pH variations were routinely observed further into the Hauraki Gulf, and especially toward the inner Firth. It was clear that carbonate conditions at the Firth were responding to more complex conditions than those for the open NE shelf, as described for other systems in proximity to the land-sea interface (Provoost et al., 2010; Joesoef et al., 2015; Rosenau et al., 2021).

Among these conditions are freshwater effects (Carstensen and Duarte, 2019; Van Dam and Wang, 2019). In all seasons the underway surveys detected increasing pCO_2 and decreasing pH from the NE shelf, through the Hauraki Gulf and into the Firth approaching its riverine inputs. These carbonate gradients correlated with decreasing salinity and TA at the head of the Firth, adjacent to its inputs of low TA and pH freshwater. However, interseasonal changes in salinity and TA were relatively slight in the Firth (maximum change ∼1.5 psu, ∼100 μmol kg^{-1} between summer and autumn in the inner Firth: **Figures 2B,F**), suggesting little potential for strong freshwater/TA effects. Accordingly, in autumn, when freshwater input was at its annual minimum and salinity and TA were at annual maxima, pCO_2 was high and pH was low, showing that the slightly increased TA was having a relatively minor buffering influence. Also, in summer and winter, when freshwater inputs were higher and TA was slightly reduced, pCO_2 was low, again indicating a minor effect of riverine carbonate inputs on Firth carbonate dynamics.

The importance of metabolism in conditioning the carbonate system was indicated by spatial variability in O_2 conditions from the outer to inner Firth. In all seasons except winter, the moored O_2 and AOU analyses showed greater O_2 undersaturation over the entire water column of the inner Firth than in the upper water column of the outer Firth, which was usually normoxic. This indicated more persistent heterotrophic metabolism throughout the water column of the inner Firth. The shoreward decreasing O_2 followed the increasing pCO_2 and decreasing pH gradients, showing that metabolic effects were having an important role in carbonate speciation, similar to results of Wallace et al. (2014) and Rheuban et al. (2019) for eastern United States estuaries and the meta-analysis of Carstensen and Duarte (2019). The increasing organic matter concentrations (chl-*a*, CDOM, turbidity, POC and DOC) from the NE shelf, through the Hauraki Gulf and the outer to inner Firth, further indicated that the shoreward increasing pCO_2 gradients were conditioned by metabolic effects.

These metabolic effects result from the interaction of terrestrial nutrient supply, primary production and respiration. GPP was nearly always greater in the inner than the outer Firth for both near-surface and deeper water depths. While the estimation of GPP from diel O_2 variations required a number of assumptions (see **Supplementary Material**), the shoreward

TABLE 2 | Inter-seasonal surface layer temperature (°C) and pCO_2 (μatm) averaged (stdev in parentheses) over inner Firth, outer Firth, Hauraki Gulf and NE shelf regions (**Figure 1B**).

	Inner Firth	Outer Firth	Hauraki Gulf	NE shelf
Spring to summer				
Initial temp	15.0 (0.1)	14.7 (0.2)	14.7 (0.2)	15.0 (0.1)
Final temp	20.6 (0.5)	20.0 (0.4)	19.9 (0.6)	20.2 (0.3)
Initial $pCO_{2,observed}$	377 (20)	372 (11)	369 (9)	367 (10)
Final $pCO_{2,observed}$	400 (21)	386 (11)	391 (20)	384 (8)
$\Delta pCO_{2,observed}$	23	14	22	17
$\Delta pCO_{2,thermal}$	96	89	86	89
$\Delta pCO_{2,biohydro}$	−63	−64	−55	−59
$\Delta pCO_{2,net}$	33	25	31	30
$\Delta pCO_{2,residual}$	−10	−11	−9	−14
Summer to autumn				
Initial temp	20.6 (0.5)	20.0 (0.4)	19.9 (0.6)	20.2 (0.3)
Final temp	21.6 (0.2)	21.6 (0.2)	21.5 (0.4)	21.0 (0.1)
Initial $pCO_{2,observed}$	400 (21)	386 (11)	391 (20)	384 (8)
Final $pCO_{2,observed}$	522 (23)	452 (28)	419 (24)	383 (8)
$\Delta pCO_{2,observed}$	122	66	28	−1
$\Delta pCO_{2,thermal}$	13	24	25	12
$\Delta pCO_{2,biohydro}$	102	36	2	−13
$\Delta pCO_{2,net}$	115	60	27	−1
$\Delta pCO_{2,residual}$	7	6	1	0
Autumn to winter				
Initial temp	21.6 (0.2)	21.6 (0.2)	21.5 (0.4)	21.0 (0.1)
Final temp	12.9 (0.5)	13.8 (0.3)	14.0 (0.5)	14.8 (0.4)
Initial $pCO_{2,observed}$	522 (23)	452 (28)	419 (24)	383 (8)
Final $pCO_{2,observed}$	384 (10)	370 (4)	363 (8)	356 (6)
$\Delta pCO_{2,observed}$	−138	−82	−56	−27
$\Delta pCO_{2,thermal}$	−157	−126	−112	−87
$\Delta pCO_{2,biohydro}$	28	59	75	74
$\Delta pCO_{2,net}$	−129	−67	−37	−13
$\Delta pCO_{2,residual}$	−9	−15	−19	−15
Winter to spring				
Initial temp	21.6 (0.2)	21.6 (0.2)	21.5 (0.4)	21.0 (0.1)
Final temp	15.0 (0.1)	14.7 (0.2)	14.7 (0.2)	15.0 (0.1)
Initial $pCO_{2,observed}$	384 (10)	370 (4)	363 (8)	356 (6)
Final $pCO_{2,observed}$	377 (20)	372 (11)	369 (9)	367 (10)
$\Delta pCO_{2,observed}$	−7	2	6	11
$\Delta pCO_{2,thermal}$	36	15	10	1
$\Delta pCO_{2,biohydro}$	−40	−14	−7	9
$\Delta pCO_{2,net}$	−4	1	3	10
$\Delta pCO_{2,residual}$	−3	0	2	1

The effects of changing temperature ($\Delta pCO_{2,thermal}$) and biological and physical factors ($\Delta pCO_{2,biohydro}$) on pCO_2 are given, along with their sum, the net interseasonal change of pCO_2 ($\Delta pCO_{2,net}$). The pCO_2 change that remained unaccounted for in the analysis was $\Delta pCO_{2,residual}$.

increasing gradient in productivity detected was consistent with higher NPP measured in the outer Firth site relative to the Hauraki Gulf (Gall and Zeldis, 2011; Bury et al., 2012). The absolute rates of GPP at the outer Firth measured by the diel method were higher than NPP predicted by a depth integrated model (Zeldis et al., 2005) and from ^{14}C uptake experiments (Gall and Zeldis, 2011) but this is expected considering likely losses to autotroph respiration. The seaward-decreasing primary production, organic matter and pCO_2 gradients were coherent with much lower riverine DIN loading to the Hauraki Gulf than to the Firth, similar to associations of high DIN loading and expressions of elevated pCO_2 and hypoxia by Wallace et al. (2014) and Rheuban et al. (2019) in eastern United States estuaries.

Drivers of the carbonate system were further resolved by the deconvolution of surface layer pCO_2 seasonal variation, combined with results from the biophysical moorings and spatial surveys. These showed how temperature interacted with metabolism (DIC uptake/release) and mixing (stratification dynamics and particle settling), to modulate pCO_2. While large increases in surface layer pCO_2 were predicted from increased temperature between spring and summer, realised pCO_2 was less, caused by reductions of surface layer DIC associated nutrient limitation and particle settling. At the inner Firth, strongly increasing pCO_2 and depressed pH and O_2 occurred between summer and autumn when temperature increase was small, but when low O_2 waters that had formed in the deeper water column were mixed toward the surface. From autumn to winter, strong pCO_2 undersaturation predicted by large temperature decrease was tempered by increased vertical mixing, weak uptake by GPP and elevated respiratory metabolism, while between winter and spring small pCO_2 increases were driven by small temperature increases and weak metabolic/mixing effects.

The effects of seasonal temperature change on pCO_2 in the deconvolution were like those seen in pCO_2 monitoring across several United States estuaries (Joesoef et al., 2015; Rosenau et al., 2021) who used similar analytical methods to separate the effects of temperature and aggregated metabolism/mixing on pCO_2. Like those studies, we did not quantitatively separate the metabolic and mixing effects. Our analysis has, however, augmented the description of those effects with observations on GPP and O_2 dynamics, and interaction of stratification, seasonal nutrient limitation and particle settling with the carbonate system. More quantitative separation of metabolic and mixing effects could be achieved by dynamic biogeochemical modelling research planned for the Hauraki Gulf/Firth system, that will deconvolve the carbonate system in greater resolution than done here, similar to Shen et al. (2019) for Chesapeake Bay (United States).

Such modelling could also resolve other potential biogeochemical effects on carbonate in addition to aerobic respiration, such as calcification, decalcification, and sulfate reduction. While these terms were shown to contribute relatively minor effects compared to aerobic respiration in Chesapeake Bay by Shen et al. (2019), TA in estuarine coastal waters can be affected by those processes, along with addition of organic matter, and nitrate uptake which contribute to the non-conservative behaviour of alkalinity (Wolf-Gladrow et al., 2007; Carstensen et al., 2018). The deconvolution did not separate out these contributions. Deviation from alkalinity – salinity relationships can be used to assess their contributions, but we consider that their contributions would not materially impact the deconvolution results we describe. The conservative behaviour of alkalinity reported here (average R^2 of the salinity/TA regressions for the 5 seasonal surveys was 0.95) suggested that the contribution of non-carbonate alkalinity was small. Furthermore, we believe that the Firth is unlikely to demonstrate

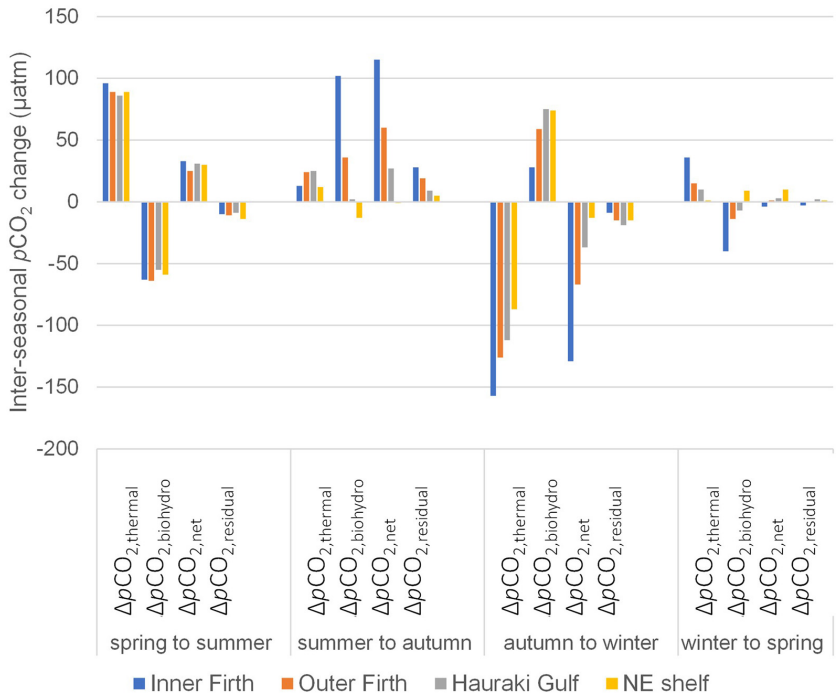

FIGURE 10 | Effects of inter-seasonal changes of surface layer temperature and combined metabolism/mixing processes, on changes of surface layer pCO_2 (µatm), for inner Firth, outer Firth, Hauraki Gulf and the NE shelf regions. Net change of pCO_2 ($\Delta pCO_{2,net}$) is the sum of temperature ($\Delta pCO_{2,thermal}$) and metabolic/mixing effects ($\Delta pCO_{2,biohydro}$). Residual change of pCO_2 ($\Delta pCO_{2,residual}$) is net change minus change in observed pCO_2 ($\Delta pCO_{2,observed}$) (**Table 2**).

TABLE 3 | Seasonal and annual averages of (A) Firth GPP, (B) ratios of C fixed within the Firth water column by GPP to total organic C loaded by rivers to the Firth.

	Spring	Summer	Autumn	Winter	Annual
(A) Firth GPP (T C y^{-1})	280683	330476	260557	171550	260817
(B) Firth GPP (T C y^{-1})/TOC river (T C y^{-1})	11	29	100	6	15

strong effects from calcification: its historic biogenic reefs (including shellfish beds) were almost completely eliminated by the late 1960's by dredge fishing and benthic habitat modification and have not returned (McLeod et al., 2012). Furthermore, the underway pCO_2 surveys surrounding the large suspended mussel farms in the eastern Firth (**Figure 2C**) showed no clear signal of pCO_2 modification in proximity to the farms, with respect to overall variability of pCO_2 over the larger Firth/Hauraki Gulf area. This was consistent with the remote sensing studies of Pinkerton et al. (2018) that showed negligible water quality (chl-*a* and turbidity) effects of those farms, arising as a consequence of their very high water flushing rates.

Water-column average variations of DIC concentration were consistent with variations of column-average net DIC flux calculated by the mass-balance analysis of Zeldis and Swaney (2018), made using nutrient, salinity and hydrometric data collected during the present study. The small inter-seasonal variation in Hauraki Gulf net DIC fluxes (**Figure 11A**) was consistent with low variation in Hauraki Gulf DIC concentrations (**Figure 11B**). Conversely, for the Firth, the wide inter-seasonal variation in net DIC fluxes reflected its larger variations in DIC concentrations. Low net DIC production in the Firth in spring (**Figure 11A**) combined with spring GPP, caused moderate DIC concentrations (**Figure 11B**). In summer, DIC increased in the lower water column and decreased in the upper column (**Figures 3C,D**) consistent with small column-averaged DIC fluxes (**Figure 11A**). In contrast, in autumn, high DIC production in the Firth generated increased DIC concentrations. In winter, high mineralisation (reflected by increased NH_4^+-N: **Figure 7D**) generated high net DIC production and concentrations.

Overall, the more variable and often high net DIC production for the Firth *vs.* the near-neutral rates for the Hauraki Gulf reflected the higher organic matter densities in the Firth and its higher nutrient loading. Together with the deconvolution and spatial survey results, the mass balance results supported our first hypothesis, that that seasonal variation in NEM is a primary determinate of carbonate and oxic responses in the Firth, but that its role in expression of high pCO_2 and reduced O_2 will be qualified by other factors, related to seasonal changes of temperature, primary production and physical structure. pCO_2 and AOU maximise in summer and autumn in the inner and outer Firth water columns, following the summer maxima of GPP at the inner Firth and settling of phytoplankton biomass in the water column along the Firth thalweg. While

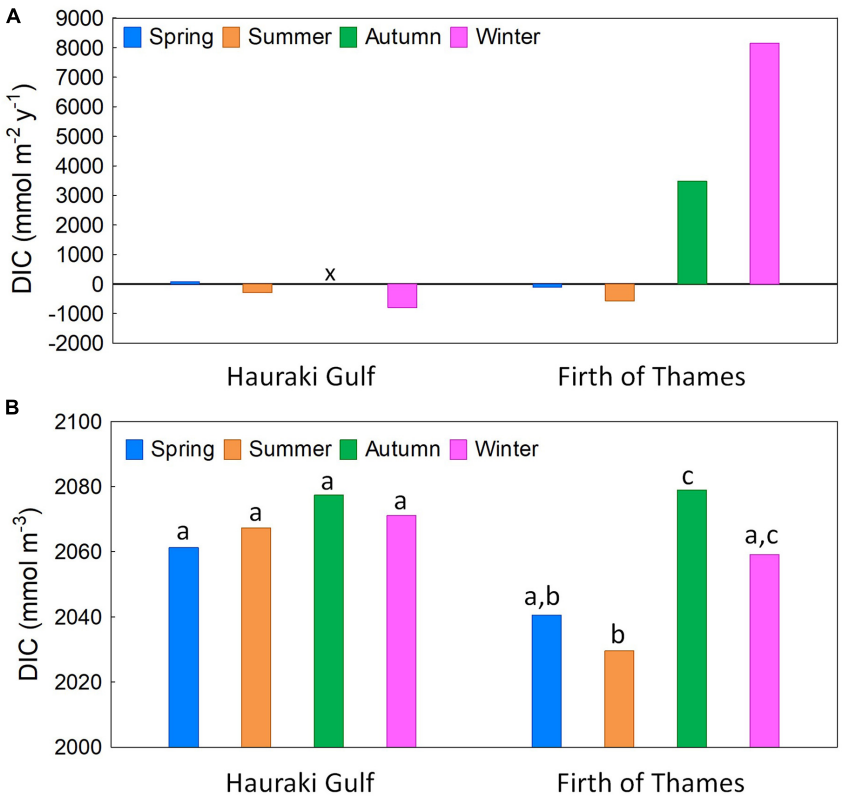

FIGURE 11 | (A) Seasonal water column-average net DIC fluxes (mmol DIC m^{-2} y^{-1}) in Hauraki Gulf and Firth of Thames regions from the mass-balance budget of Zeldis and Swaney (2018) (see **Figure 1B** for mass balance box delineations). The mass balance estimate for the Hauraki Gulf in autumn ("x") could not be calculated (Zeldis and Swaney, 2018). **(B)** Seasonal water column-average DIC concentrations (mmol DIC m^{-3}) in Hauraki Gulf and Firth regions from the present study. Within each region, seasonal concentrations with different letters were significantly different ($p < 0.05$; Neuman-Keuls multiple comparisons).

the production/respiration cycle is a continuous process in all seasons, its balance varies (Kemp et al., 1997; Sunda and Cai, 2012), with system DIC fluxes near neutral under high GPP and temperature increases in spring to summer but swinging toward net-respiratory metabolism in autumn, when the stressors of acidification and hypoxia are most strongly expressed. The results reflect the conclusion of Carstensen and Duarte (2019) that pH variability is pronounced in coastal systems with strong decoupling of production and respiration processes, in our case through both seasonal and stratification effects.

The late seasonal onset of net-heterotrophy is a consistent event in the Firth in summer and autumn, as reflected by depressed O_2 in those seasons in the 15-year O_2 sampling series of Zeldis and Swaney (2018) at the outer Firth site. That time-series shows interannual variation, however, and our results also showed variation in intensity of pH and O_2 depression between autumn 2010 and autumn 2013. This variation likely arose from an interplay of factors, including the greater chl-*a* and phaeo-*a* biomasses and more intense stratification in 2010 than 2013. These interactions resembled those in several eastern United States estuaries including Chesapeake Bay (Kemp et al., 1992; Kemp et al., 2005; Scully, 2016) and Narragansett Bay (Wallace et al., 2014) where seasonal stratification is a necessary (but not sufficient) driver of low O_2. The onset of seasonal hypoxia in Chesapeake Bay is set by the timing of seasonal physical stratification, but the severity and extent of hypoxia is a consequence of its interaction with the production cycle including eutrophication effects (Hagy et al., 2004).

Origin of Organic Matter Driving Metabolism

The Firth system maintained NEM near equilibrium in spring and summer (**Figure 11A**) but expressed high net DIC production in autumn and winter. The finding that high DIC production occurred after riverine organic matter inputs had fallen to their lowest annual values in autumn was not consistent with other studies associating heterotrophic metabolism with riverine allochthonous organic loading in coastal systems, including Salisbury et al. (2008) who found that riverine organic carbon inputs drove pCO_2 supersaturation in two eastern United States estuaries. Unlike those systems, there was evidence in the Firth that the organic matter underpinning its autumn respiratory maximum was predominately autochthonous and derived from *in situ* primary production, rather than imported from catchments. The median molar POC:PON composition of suspended matter in the Firth was 6.6 with relatively little seasonal or spatial range [i.e., equal to the canonical Redfield

ratio for marine phytoplankton (Redfield et al., 1963)], and was well below POC:PON expected for terrigenous organic matter ($\geq$ 20) (Ruttenberg and Goñi, 1997; Meyers and Teranes, 2001; Bianchi, 2007). This suggested that its source was dominated by marine phytoplankton. The median molar DOC:DON of dissolved organic matter in the Firth water column was 11.6, higher than that of the particulate matter, but still well below that expected for terrigenous organic matter. The greater C:N in the dissolved than the particulate matter could have been due to the tendency of N to be scavenged preferentially with respect to C in marine organic matter as it is mineralised (Bianchi, 2007).

Further evidence for the dominance of an autochthonous source of organic matter driving Firth metabolism is as follows. About ∼80% of the riverine N entering the Firth is DIN, while the remainder is a mixture of PON and DON (derived from **Figure 4B**). The C:N of organic matter in river water entering the Firth is not known (S. Elliott, NIWA pers.comm. April 2021), but if it is assumed that an approximate molar C:N for terrigenous organic matter delivered by river water is 20 (see above), the C added to the system by river input (i.e., allochthonous C inputs) can be calculated from the riverine organic N inputs. This can then be compared with carbon fixation by GPP within the Firth to gain a perspective on the size of the terrigenous organic C load compared to the autochthonous organic C input from GPP (**Table 3A**). The very high ratios of autochthonous to allochthonous C inputs (**Table 3B**) in summer (29-fold) and especially autumn (100-fold) support the suggestion from molar C:N ratios (above), that the dominant source of organic matter in the Firth was autochthonous production by phytoplankton, with allochthonous inputs being very small in comparison. In winter, the ratio was smaller (6-fold) and mineralisation of organic matter was evident from elevated levels of NH_4^+-N and DIC production. Potentially, organic matter supplied from the catchment may have been playing a larger role in winter, although low temperatures and winter mixing counteracted those effects, resulting in undersaturated pCO_2.

The riverine mean annual areal TOC load calculated for the Firth was 16 T C km^{-2} y^{-1}, more than 2 orders lower than the annual areal TOC loads to the much smaller estuarine systems studied by Salisbury et al. (2008) (derived from their Tables 2, 3). Caffrey (2004) described NEM across 22 United States estuaries and concluded that estuarine surface area was a significant factor explaining variability in NEM; larger systems were closer to balance than smaller, shallow systems that were supplied with greater allochthonous organic matter. It is therefore likely that estuary size and depth, as well as ratio of allochthonous to autochthonous organic load, underlies differences in sources of organic matter driving metabolism.

The Firth was found to generate much larger amounts of organic C *via* GPP than it imported as riverine organic C. However, as described above (Introduction), rivers dominate the input of DIN to the Firth and are thus primarily responsible for fuelling the generation of the organic matter. The results therefore support our second hypothesis, that the organic matter involved in metabolism will be supplied primarily by fixation within the Firth system, rather than imported from the catchment, and will be driven by supply of riverine DIN.

The results indicated that a mechanistic connection exists between spring and summer GPP maxima in the upper water column and increased lower water column heterotrophic metabolism in summer and autumn, with the linkage related to seasonal stratification nutrient limitation, settlement and mineralisation of phytoplankton, as proposed by Paerl (2006) and Sunda and Cai (2012) to explain hypoxia and acidification of coastal bottom waters. The expression of late-season acidification and hypoxia has likely increased with enhanced GPP in the Firth over the history of its catchment land-use intensification and increased N loading [*ca* 82% over natural levels (Snelder et al., 2017): Introduction]. Our results support the findings of Carstensen and Duarte (2019) who distinguished well-mixed systems where enhanced primary production can act to counter ocean acidification (Borges and Gypens, 2010; Provoost et al., 2010), from seasonal, stratifying systems, where eutrophication can promote acidification when carbon is respired at the end of the production season (Sunda and Cai, 2012).

As well as exhibiting seasonal patterns in NEM and vertical stratification, the dynamics in the Firth may have an important horizontal component. A conceptual model of this within the Firth estuarine circulation system is as follows. The biomass fixed in the productive inner Firth is advected toward the outer Firth, in its seaward surface estuarine circulation. During transit, it undergoes nutrient limitation, sinking and mineralisation, forming O_2-depleted waters at depth. These deep waters recirculate back toward the inner Firth in the estuarine return circulation. Such two-layer circulation has been shown for the Firth (Zeldis et al., 2010; O'Callaghan and Stevens, 2017) supporting this recirculation mechanism. These dynamics may explain the persistent positive AOU, intense O_2 depletion and low pH displayed at the inner Firth, despite its high GPP. A similar recirculation mechanism was described for Chesapeake Bay by Moriarty et al. (2020) to explain observations of persistent low O_2 conditions in the mid- to inner-estuary. The validity of this conceptual model for the Firth could be tested with dynamic biogeochemical modelling like that applied by those authors.

Implications for Coastal Resource Management

Prior to the present study and that of Zeldis and Swaney (2018), the response of the Firth carbonate and oxic systems to its history of nutrient enrichment was unknown. These studies have shown the susceptibility of the Firth to acidification and hypoxia and its forcing by catchment DIN loading. Deep, long residence time estuaries that seasonally stratify, such as the Firth, appear to be susceptible, as evidenced here by the high levels of AOU that are occurring at only moderate chl-*a* levels. Chl-*a* at the inner Firth site from 2015 to 2017 during 3-monthly seasonal surveys had mean 6.0 mg chl-*a* m^{-3} and 90^{th} percentile value 22.2 mg chl-*a* m^{-3} (authors' unpubl. NIWA data). This resembles conditions in Chesapeake Bay, where intense pH depression and hypoxia (Shen et al., 2019) were accompanied by mean chl-*a* levels in its mesohaline reaches of about 8 mg chl-*a* m^{-3} (Kemp et al., 2005) and recommended 90^{th} percentile management threshold values that 'should rarely be exceeded' ranged from

6.9 to 27 mg chl-*a* m^{-3} (Harding et al., 2014). In their meta-analysis of areal TN loading rates to estuaries, Boynton and Kemp (2008) found that Chesapeake Bay was near the lower end of their loading frequency distribution. Many other estuaries had much higher areal loadings, yet Chesapeake Bay is regarded as an iconic example of severe environmental degradation driven by anthropogenic nutrient loading (Kemp et al., 1997, 2005). It is likely that the physiography of Chesapeake Bay (relatively clear waters, long residence times, seasonal stratification) renders it susceptible to eutrophication, and its similarity in those respects with the Firth suggests why the Firth is also. While N loading to Chesapeake Bay (∼14 g TN m^{-2} y^{-1}) is about twice that for the inner Firth (∼7.3 g TN m^{-2} y^{-1}), and its pH and O_2 depression are more severe, the systems appear to share this sensitivity to these physiographic features in expression of acidification and hypoxia.

The present results show that the Firth displays significantly depressed pH and O_2 in concert with seasonal occurrence of heterotrophic NEM, reaching pH levels below ∼7.8 and O_2 levels below ∼150 μmol kg^{-1} (∼4.8 mg L^{-1}) in summer and autumn (**Figures 9E,C**). To put these conditions in perspective, the review of Gazeau et al. (2013) documented responses of adult and larval/juvenile shelled molluscs pH decreases of ≤0.4 units, and found that while adults showed few negative responses, larval stages were much more vulnerable to acidification stress. Recent review of acidification effects on crustacea (Bednaršek et al., 2021) found frequent negative effects on adults and larval/juvenile stages to pH reductions ≤ 0.4, and experiments on decapod larvae combining acidification and hypoxia (Tomasetti et al., 2021) have demonstrated potential for severe synergistic effects over short exposure time scales. For New Zealand taxa, Law et al. (2018) found that acidification levels we show for the Firth approached deleterious levels for macroalgae (corallines), and early life stages of sea urchins, sand dollars, abalone and New Zealand Greenshell® mussels, which are grown in the large mussel farms in the Firth (Law et al., 2019).

In terms of O_2 stress, the observations are valuable for finfish aquaculture management in the Firth, where a tenderer has obtained the right to apply for resource consent to farm yellowtail kingfish (*Seriola lalandi*) at a site ∼2.5 km SE of the outer Firth mooring of our study (Conomos, 2018).[1] Kingfish juveniles show strongly impaired growth rates (39%) in low O_2 treatments ranging between 2.9 and 4.9 mg O_2 L^{-1} (Bowyer et al., 2014), and significantly reduced nutrient utilisation at 5.4 mg O_2 L^{-1} (Pirozzi et al., 2019). Summer and autumn O_2 levels were frequently at or below those levels in the lower water column of the outer Firth area (∼4.8 mg O_2 L^{-1}). The extent to which those suboxic waters would intersect the kingfish farm cages in the upper water column will need careful evaluation. Also, local regional coastal planning (Environment Waikato Policy, and Strategy Group, 2012) provides for a potential discharge from fish farming of 1,100 t TN y^{-1} over the inner and outer Firth areas, which is ∼27% of the TN load currently input by the Firth's rivers [∼4100 t TN y^{-1}; derived from Zeldis and Swaney (2018)]. How this additional loading would interact with the Firth's carbonate and oxic conditions will need careful evaluation, including how its products would be transported within the Firth's estuarine circulation.

The observations of the present study have stimulated and informed new research by resource managers and scientists that integrates dynamic ocean biogeochemical models with catchment land-use and runoff models. The study shows how such multi-faceted coastal observations may be used to understand coastal ecosystem state, and to parameterise dynamic modelling to manage coastal resource use and forecast catchment nutrient limit settings required to preserve ecosystem health.

[1]Fish farm a step closer | Hauraki Gulf Forum Fish farm a step closer (gulfjournal.org.nz).

DATA AVAILABILITY STATEMENT

The original contributions presented in the study are included in the article/**Supplementary Material**, further inquiries can be directed to the corresponding author.

AUTHOR CONTRIBUTIONS

JZ and KC conceived the research. JZ led the writing and field surveys. KC led the carbonate sampling and analysis. SG conceived and executed the diel GPP analysis. MG analysed the INF data, and designed shipboard data acquisition systems. All authors contributed to the article and approved the submitted version.

FUNDING

Project support was from the New Zealand Ministry of Business, Innovation and Employment (MBIE)-funded "Coasts and Oceans" Outcome-Based Investment contract C01X0501, NIWA Strategic Science Investment Fund project "Ocean Flows and Productivity" (COOF2202), and "Coastal Acidification-Rates, Impacts and Management" contract C01X1510. Funds for open access fees were from 'Ocean Flows and Productivity' (COOF2202) and 'Ocean-Climate Interactions' (CAOC2201).

ACKNOWLEDGMENTS

We thank scientific staff and crews of NIWA R.V.s *Kaharoa* and *Rangitahi* III, and Western Work Boats *Star Keys*, who enabled the ocean-going data. At NIWA we thank the Chemistry Laboratory for sample analysis, Jochen Bind for database administration and Scott Nodder for manuscript review.

SUPPLEMENTARY MATERIAL

The Supplementary Material for this article can be found online at: https://www.frontiersin.org/articles/10.3389/fmars.2021.803439/full#supplementary-material

REFERENCES

Anderson, L. A. (1995). On the hydrogen and oxygen content of marine phytoplankton. *Deep Sea Res. 1 Oceanogr. Res. Pap.* 42, 1675–1680. doi: 10.1016/0967-0637(95)00072-E

Barton, A., Hales, B., Waldbusser, G., Langdon, C., and Feely, R. (2012). The Pacific oyster, *Crassostrea gigas*, shows negative correlation to naturally elevated carbon dioxide levels: implications for near-term ocean acidification effects. *Limnol. Oceanogr.* 57, 698–710. doi: 10.4319/lo.2012.57.3.0698

Bednaršek, N., Ambrose, R., Calosi, P., Childers, R. K., Feely, R. A., Litvin, S. Y., et al. (2021). Synthesis of thresholds of ocean acidification impacts on decapods. *Front. Mar. Sci.* 8:1542. doi: 10.3389/fmars.2021.651102

Bianchi, T. S. (2007). *Biogeochemistry of Estuaries*. Oxford: Oxford University Press. doi: 10.1093/oso/9780195160826.001.0001

Borges, A. V., and Gypens, N. (2010). Carbonate chemistry in the coastal zone responds more strongly to eutrophication than ocean acidification. *Limnol. Oceanogr.* 55, 346–353. doi: 10.4319/lo.2010.55.1.0346

Bowyer, J. N., Booth, M. A., Qin, J. G., D'Antignana, T., Thomson, M. J. S., and Stone, D. A. J. (2014). Temperature and dissolved oxygen influence growth and digestive enzyme activities of yellowtail kingfish Seriola lalandi (Valenciennes, 1833). *Aquac. Res.* 45, 2010–2020. doi: 10.1111/are.12146

Boynton, W., and Kemp, W. (2008). "Estuaries," in *Nitrogen in the Marine Environment*, 2nd Edn, eds D. Capone, D. Bronk, M. Mulholland, and E. Carpenter (Burlington, MA: Elsevier), 809–856. doi: 10.1016/B978-0-12-372522-6.00018-9

Bury, S. J., Zeldis, J. R., Nodder, S. D., and Gall, M. (2012). Regenerated primary production dominates in a periodically upwelling shelf ecosystem, northeast New Zealand. *Cont. Shelf Res.* 32, 1–21. doi: 10.1016/j.csr.2011.09.008

Caffrey, J. (2004). Factors controlling net ecosystem metabolism in U.S. estuaries. *Estuaries* 27, 90–101. doi: 10.1007/BF02803563

Caffrey, J., Murrell, M., Amacker, K., Harper, J., Phipps, S., and Woodrey, M. (2014). Seasonal and inter-annual patterns in primary production, respiration, and net ecosystem metabolism in three Estuaries in the northeast Gulf of Mexico. *Estuaries Coasts* 37, 222–241. doi: 10.1007/s12237-013-9701-5

Carstensen, J., Chierici, M., Gustafsson, B. G., and Gustafsson, E. (2018). Long-term and seasonal trends in estuarine and coastal carbonate systems. *Glob. Biogeochem. Cycles* 32, 497–513. doi: 10.1002/2017gb005781

Carstensen, J., and Duarte, C. M. (2019). Drivers of pH variability in coastal ecosystems. *Environ. Sci. Technol.* 53, 4020–4029. doi: 10.1021/acs.est.8b03655

Chamberlin, W. S., Booth, C. R., Kieffer, D. A., Morrow, J. H., and Murphy, R. C. (1990). Evidence for a simple relationship between natural fluorescence, photosynthesis and chlorophyll in the sea. *Deep Sea Res. A Oceanogr. Res. Pap.* 37, 951–973. doi: 10.1016/0198-0149(90)90105-5

Conomos, K. (2018). *Fish Farm a Step Closer. Hauraki Gulf Forum*. Available online at: https://gulfjournal.org.nz/article/fish-farm-a-step-closer/ (accessed December 20, 2021).

Cox, T. J. S., Maris, T., Soetaert, K., Kromkamp, J. C., Meire, P., and Meysman, F. (2015). Estimating primary production from oxygen time series: a novel approach in the frequency domain. *Limnol. Oceanogr. Methods* 13, 529–552. doi: 10.1002/lom3.10046

Dickson, A., and Millero, F. (1987). A comparison of the equilibrium constants for the dissociation of carbonic acid in seawater media. *Deep Sea Res.* 34, 1733–1743. doi: 10.1016/0198-0149(87)90021-5

Dickson, A., Sabine, C., and Christian, J. (2007). *Guide to Best Practices for Ocean CO_2 Measurements, in PICES Special Publication 3 IOCCP Report*. Sidney, BC: North Pacific Marine Science Organization.

Duarte, C., Hendriks, I., Moore, T., Olsen, Y., Steckbauer, A., Ramajo, L., et al. (2013). Is ocean acidification an open-ocean syndrome? Understanding anthropogenic impacts on seawater pH. *Estuaries Coasts* 36, 221–236. doi: 10.1007/s12237-013-9594-3

Duarte, C. M., and Prairie, Y. T. (2005). Prevalence of heterotrophy and atmospheric CO_2 emissions from aquatic ecosystems. *Ecosystems* 8, 862–870. doi: 10.1007/s10021-005-0177-4

Environment Waikato Policy, and Strategy Group (2012). *Waikato Regional Coastal Plan*. Waikato Regional Council Document Number 2181758. Available online at: https://www.waikatoregion.govt.nz/assets/WRC/Council/Policy-and-Plans/Rules-and-regulation/Waikato-Regional-Coastal-Plan-October-2011.pdf (accessed December 20, 2012)

Gall, M., and Zeldis, J. (2011). Phytoplankton biomass and primary production responses to physico-chemical forcing across the northeastern New Zealand continental shelf. *Cont. Shelf Res.* 31, 1799–1810. doi: 10.1016/j.csr.2011.06.003

Gazeau, F., Parker, L., Comeau, S., Gattuso, J.-P., O'Connor, W., Martin, S., et al. (2013). Impacts of ocean acidification on marine shelled molluscs. *Mar. Biol.* 160, 2207–2245. doi: 10.1007/s00227-013-2219-3

Gobler, C. J., DePasquale, E. L., Griffith, A. W., and Baumann, H. (2014). Hypoxia and acidification have additive and synergistic negative effects on the growth, survival, and metamorphosis of early life stage bivalves. *PLoS One* 9:e83648. doi: 10.1371/journal.pone.0083648

Hagy, J., Boynton, W., Keefe, C., and Wood, K. (2004). Hypoxia in Chesapeake Bay, 1950-2001: long-term change in relation to nutrient loading and river flow. *Estuaries* 27, 634–658. doi: 10.1007/BF02907650

Harding, L. W. Jr., Batiuk, R. A., Fisher, T. R., Gallegos, C. L., Malone, T. C., Miller, W. D., et al. (2014). Scientific bases for numerical chlorophyll criteria in Chesapeake Bay. *Estuaries Coasts* 37, 134–148. doi: 10.1007/s12237-013-9656-6

Joesoef, A., Huang, W. J., Gao, Y., and Cai, W. J. (2015). Air–water fluxes and sources of carbon dioxide in the Delaware Estuary: spatial and seasonal variability. *Biogeosciences* 12, 6085–6101. doi: 10.5194/bg-12-6085-2015

Judd, W. (2015). Natural values. *N. Z. Geogr.* 133, 36–61.

Kelly, S., Kirikiri, R., Sim-Smith, C., and Lee, S. (2020). *State of our Gulf 2020: Hauraki Gulf/Tīkapa Moana/Te Moana-nui-a-Toi State of the Environment Report 2020*. Auckland: Hauraki Gulf Forum.

Kemp, W., Boynton, W. R., Adolfi, J. E., Boesch, D. F., Boicourt, W. C., Brush, G., et al. (2005). Eutrophication of Chesapeake Bay: historical trends and ecological interactions. *Mar. Ecol. Prog. Ser.* 303, 1–29. doi: 10.3354/meps303001

Kemp, W. M., Sampou, P. A., Garber, J., Tuttle, J., and Boynton, W. R. (1992). Seasonal depletion of oxygen from bottom waters of Chesapeake Bay: roles of benthic and planktonic respiration and physical exchange processes. *Mar. Ecol. Prog. Ser.* 85, 137–152. doi: 10.3354/meps085137

Kemp, W., Smith, E., Marvin-DiPasquale, M., and Boynton, W. (1997). Organic carbon balance and net ecosystem metabolism in Chesapeake Bay. *Mar. Ecol. Prog. Ser.* 150, 229–248. doi: 10.3354/meps150229

Lachat (2010). *Methods List for Automated Ion Analyzers*. Available online at: http://www.lachatinstruments.com/download/LL022-Methods-List_5-10.pdf (accessed December 20, 2021)

Law, C. S., Bell, J. J., Bostock, H. C., Cornwall, C. E., Cummings, V. J., Currie, K., et al. (2018). Ocean acidification in New Zealand waters: trends and impacts. *N. Z. J. Mar. Freshw. Res.* 52, 155–195. doi: 10.1111/gcb.15899

Law, C. S., Zeldis, J. R., Bostock, H., Cummings, V., Currie, K., Frontin-Rollet, G., et al. (2019). *A Synthesis of New Zealand Ocean Acidification Research, with Relevance to the Hauraki Gulf*. NIWA Client Report 2019165WN. Auckland: National Institute of Water & Atmospheric Research Ltd, 77.

McLeod, I. M., Parsons, D. M., Morrison, M. A., Le Port, A., and Taylor, R. B. (2012). Factors affecting the recovery of soft-sediment mussel reefs in the Firth of Thames, New Zealand. *Mar. Freshw. Res.* 63, 78–83. doi: 10.1071/MF11083

Mehrbach, C., Culberson, C. H., Hawley, J. E., and Pytkowicz, R. M. (1973). Measurement of the apparent dissociation constants of carbonic acid in seawater at atmospheric pressure. *Limnol. Oceanogr.* 19, 897–907. doi: 10.4319/lo.1973.18.6.0897

Meyers, P. A., and Teranes, J. L. (2001). "Sediment organic matter," in *Tracking Environmental Change Using Lake Sediments*, eds W. M. Last and J. P. Smol (Dordrecht: Kluwer Academic Publishers), 239–269. doi: 10.1007/0-306-47670-3_9

Moriarty, J. M., Friedrichs, M. A. M., and Harris, C. K. (2020). Seabed resuspension in the Chesapeake Bay: implications for biogeochemical cycling and hypoxia. *Estuaries Coasts* 44, 103–122. doi: 10.1007/s12237-020-00763-8

NRC (2000). *Clean Coastal Waters Understanding and Reducing the Effects of Nutrient Pollution*. Washington DC: National Academy Press.

O'Boyle, S., McDermott, G., Noklegaard, T., and Wilkes, R. (2013). A simple index of trophic status in estuaries and coastal bays based on measurements of pH and dissolved oxygen. *Estuaries Coasts* 36, 158–173. doi: 10.1007/s12237-012-9553-4

O'Callaghan, J. M., and Stevens, C. L. (2017). Evaluating the surface response of discharge events in a New Zealand Gulf-ROFI. *Front. Mar. Sci.* 4:232. doi: 10.3389/fmars.2017.00232

Osma, N., Latorre-Melín, L., Jacob, B., Contreras, P. Y., von Dassow, P., and Vargas, C. A. (2020). Response of phytoplankton assemblages from naturally acidic

coastal ecosystems to elevated pCO_2. *Front. Mar. Sci.* 7:323. doi: 10.3389/fmars.2020.00323

Paerl, H. W. (2006). Assessing and managing nutrient-enhanced eutrophication in estuarine and coastal waters: interactive effects of human and climatic perturbations. *Ecol. Eng.* 26, 40–54. doi: 10.1016/j.ecoleng.2005.09.006

Parsons, D. M., Hartill, B. W., Broekhuizen, N., McKenzie, J. R., Stephenson, F., Petersen, G. L., et al. (2021). Integrating multi-disciplinary data sources relating to inshore fisheries management *via* a Bayesian network. *Ocean Coast. Manag.* 208, 105636. doi: 10.1016/j.ocecoaman.2021.105636

Peart, R. (2016). *The Story of the Hauraki Gulf: Discovery, Transformation, Restoration*. Auckland: David Bateman Limited.

Pinkerton, M., Gall, M., Wood, S., and Zeldis, J. (2018). Measuring the effects of bivalve mariculture on water quality in northern New Zealand using 15 years of MODIS-Aqua satellite observations. *Aquac. Environ. Interact.* 10, 529–545. doi: 10.3354/aei00288

Pirozzi, I., Benito, M. R., and Booth, M. (2019). Protein, amino acid and energy utilisation of juvenile Yellowtail Kingfish (*Seriola lalandi*): quantifying abiotic influences. *Aquaculture* 513, 734439. doi: 10.1016/j.aquaculture.2019.734439

Provoost, P., van Heuven, S., Soetaert, K., Laane, R. W. P. M., and Middelburg, J. J. (2010). Seasonal and long-term changes in pH in the Dutch coastal zone. *Biogeosciences* 7, 3869–3878. doi: 10.1111/jpy.12893

RCoreTeam (2014). *GPPFourier: Calculate Gross Primary Production (GPP) from O_2 Time Series Version 2.1 from CRAN (rdrr.io)*. Available online at: https://rdrr.io/cran/GPPFourier/ (accessed December 20, 2021).

Redfield, A. C., Ketchum, B. H., and Richards, F. A. (1963). "The influence of organisms on the composition of seawater," in *The Sea*, ed. M. N. Hill (New York, NY: Wiley & Sons), 26–77.

Rheuban, J. E., Doney, S. C., McCorkle, D. C., and Jakuba, R. W. (2019). Quantifying the effects of nutrient enrichment and freshwater mixing on coastal ocean acidification. *J. Geophys. Res. Ocean.* 124, 9085–9100. doi: 10.1029/2019jc015556

Rosenau, N. A., Galavotti, H., Yates, K. K., Bohlen, C. C., Hunt, C. W., Liebman, M., et al. (2021). Integrating high-resolution coastal acidification monitoring data across seven united states estuaries. *Front. Mar. Sci.* 8:1066. doi: 10.3389/fmars.2021.679913

Ruttenberg, K. C., and Goñi, M. A. (1997). Phosphorus distribution, elemental ratios, and stable carbon isotopic composition of arctic, temperate, and tropical coastal sediments: tools for characterizing bulk sedimentary organic matter. *Mar. Geol.* 139, 123–145. doi: 10.1016/S0025-3227(96)00107-7

Salisbury, J. E., Vandemark, D., Hunt, C. W., Campbell, J. W., McGillis, W. R., and McDowell, W. H. (2008). Seasonal observations of surface waters in two Gulf of Maine estuary-plume systems: relationships between watershed attributes, optical measurements and surface pCO_2. *Estuar. Coast. Shelf Sci.* 77, 245–252. doi: 10.1016/j.ecss.2007.09.033

Schlitzer, R. (2013). *Ocean Data View*. Available online at: http://odv.awi.de (accessed December 20, 2021)

Scully, M. E. (2016). The contribution of physical processes to inter-annual variations of hypoxia in Chesapeake Bay: a 30-yr modeling study. *Limnol. Oceanogr.* 61, 2243–2260. doi: 10.1002/lno.10372

Shen, C., Testa, J. M., Li, M., Cai, W.-J., Waldbusser, G. G., Ni, W., et al. (2019). Controls on carbonate system dynamics in a coastal plain estuary: a modeling study. *J. Geophys. Res. Biogeosci.* 124, 1–18. doi: 10.1029/2018JG004802

Snelder, T. H., Larned, S. T., and McDowell, R. W. (2017). Anthropogenic increases of catchment nitrogen and phosphorus loads in New Zealand. *N. Z. J. Mar. Freshw. Res.* 52, 1–26. doi: 10.1021/acs.est.9b03120

Sunda, W., and Cai, W.-J. (2012). Eutrophication induced CO_2-acidification of subsurface coastal waters: interactive effects of temperature, salinity and atmospheric pCO_2. *Environ. Sci. Technol.* 46, 10651–10659. doi: 10.1021/es300626f

Testa, J., Clark, J., Dennison, W., Donovan, E., Fisher, A., Ni, W., et al. (2017). Ecological forecasting and the science of hypoxia in Chesapeake Bay. *BioScience* 67, 614–626. doi: 10.1002/eap.2384

Tomasetti, S. J., Kraemer, J. R., and Gobler, C. J. (2021). Brief episodes of nocturnal hypoxia and acidification reduce survival of economically important blue crab (*Callinectes sapidus*) Larvae. *Front. Mar. Sci.* 8:1190. doi: 10.3389/fmars.2021.720175

Van Dam, B. R., and Wang, H. (2019). Decadal-scale acidification trends in adjacent North Carolina estuaries: competing role of anthropogenic CO_2 and riverine alkalinity loads. *Front. Mar. Sci.* 6:136. doi: 10.3389/fmars.2019.00136

Vant, B. (2011). *Water Quality of the Hauraki Rivers and Southern Firth of Thames, 2000–09*. Waikato Regional Council Technical Report 2011/06. Hamilton: Waikato Regional Council, 32.

Vant, B. (2016). *Water Quality and Sources of Nitrogen and Phosphorus in the Hauraki Rivers, 2006–15. Waikato Regional Council Technical Report 2016/17*. Hamilton: Waikato Regional Council, 29.

Wallace, R. B., Baumann, H., Grear, J. S., Aller, R. C., and Gobler, C. J. (2014). Coastal ocean acidification: the other eutrophication problem. *Estuar. Coast. Shelf Sci.* 148, 1–13. doi: 10.1371/journal.pone.0202093

Wolf-Gladrow, D. A., Zeebe, R. E., Klaas, C., Körtzinger, A., and Dickson, A. G. (2007). Total alkalinity: the explicit conservative expression and its application to biogeochemical processes. *Mar. Chem.* 106, 287–300. doi: 10.1016/j.marchem.2007.01.006

Zeldis, J., Stewart, C., Walkington, M., Bind, J., and Diettrich, J. (2010). *NIWA Firth of Thames Monitoring Mooring Summary Data Report*. NIWA Client Report CHC2010-134. Auckland: National Institute of Water and Atmospheric Research, 17.

Zeldis, J., Swales, A., Currie, K., Safi, K., Nodder, S., Depree, C., et al. (2015). *Firth of Thames Water Quality and Ecosystem Health – Data Report*. NIWA Client Report CHC2014-123. Auckland: National Institute of Water and Atmospheric Research, 177.

Zeldis, J. R., and Francis, R. I. C. C. (1998). A daily egg production method estimate of snapper biomass in Hauraki Gulf, New Zealand. *ICES J. Mar. Sci. J. Conseil* 55, 522–534. doi: 10.1006/jmsc.1997.0277

Zeldis, J. R., Oldman, J., Ballara, S. L., and Richards, L. A. (2005). Physical fluxes, pelagic ecosystem structure, and larval fish survival in Hauraki Gulf, New Zealand. *Can. J. Fish. Aquat. Sci.* 62, 593–610. doi: 10.1139/f04-209

Zeldis, J. R., and Swaney, D. P. (2018). Balance of catchment and offshore nutrient loading and biogeochemical response in four New Zealand coastal systems: implications for resource management. *Estuaries Coasts* 41, 2240–2259. doi: 10.1007/s12237-018-0432-5

Zeldis, J. R., and Willis, K. J. (2015). Biogeographic and trophic drivers of mesozooplankton distribution on the northeast continental shelf and in Hauraki Gulf, New Zealand. *N. Z. J. Mar. Freshw. Res.* 49, 69–86. doi: 10.1080/00288330.2014.955806

Conflict of Interest: The authors declare that the research was conducted in the absence of any commercial or financial relationships that could be construed as a potential conflict of interest.

Publisher's Note: All claims expressed in this article are solely those of the authors and do not necessarily represent those of their affiliated organizations, or those of the publisher, the editors and the reviewers. Any product that may be evaluated in this article, or claim that may be made by its manufacturer, is not guaranteed or endorsed by the publisher.